coatings

MDPI

Article

Rheological Enhancement of Bitumen Through Valorisation of Organic Waste Additives for Enhanced Railway Track Performance at Medium and High Temperatures

Filippo Giammaria Praticò [1], Ezgi Eren [2] and Vamsi Navya Krishna Mypati [1,*]

[1] DIIES Department, University "Mediterranea" of Reggio Calabria, Via Zehender, 89122 Reggio Calabria, Italy; filippo.pratico@unirc.it
[2] Civil Engineering Department, Faculty of Engineering, Adana Alparslan Turkes Science and Technology University, 01250 Adana, Turkey; eeren@atu.edu.tr
* Correspondence: vamsi.mypati@unirc.it

Abstract

In railway engineering, waterproofing layers (or blankets), composed of bitumen and mineral aggregates, are a viable and promising solution, but further innovation is needed to achieve higher mechanical characteristics and a better balance between virgin and recycled materials. Based on the above, this study investigates the potential improvements in rheological properties of a railway-oriented hard bitumen, HD, modified with a ternary system consisting of an organic compound (OC), a multifunctional additive (MA), and a modified fibrous additive (MFA) obtained from the utilisation of organic waste. In this context, comprehensive empirical, rheological, and chemical tests were performed on reference and modified bituminous blends. Results confirmed that a synergistic blend of 0.5% MA, 2% OC, and 3% MFA achieved a high R% (93.99) and G*, as well as minimal Jnr, which resulted in the best rank. This ternary combination increased viscosity by 124.97% at 150 °C, improved rutting resistance by 60.69%, and improved binder-level fatigue indicator (G*sinδ) by 45.40% under the unaged DSR sweep conditions. A mechanistic interpretation was provided. These findings support the use of OC, MA, and MFA as sustainable modifiers to enhance the high-temperature rheological performance of HD binders for railway waterproofing layers and sub-ballast applications. Future research should evaluate (1) long-term field performance and compatibility with ballast and subgrade materials, and (2) moisture damage resistance. Indeed, this cannot be inferred from binder rheology alone and should be verified through mixture-level moisture susceptibility and binder–aggregate adhesion tests.

Keywords: rheological properties; bitumen modification; rutting; fatigue; organic additive; multifunctional additive; railway; waterproofing layer

Academic Editors: Yongcheng Ji and Vasileios Koutsos

Received: 16 December 2025
Revised: 20 January 2026
Accepted: 3 February 2026
Published: 5 February 2026

1. Introduction

Passenger and freight demand for rail transportation continues to rise, prompting many railways to increase axle loads and speeds. When axle loads exceed 25 t/axle, the dynamic stresses on the track components intensify, causing conventional ballast–subgrade systems to experience rapid settlement and structural degradation [1]. Consequently, there is renewed interest in asphalt track systems, which use bituminous sub-ballast and waterproofing layers to distribute loads more uniformly and provide moisture isolation. Improved modified asphalt mixtures and multifunctional additives have played a decisive

role in revitalising asphalt track research; Na, et al. [2] observed that the popularity of asphalt tracks has increased as additives and modifiers have become widely available, offering improved fatigue and rutting performance relative to unmodified asphalt. The present manuscript, therefore, focuses on rheological enhancement of bitumen specifically for railway track applications.

Although asphalt sub-ballast layers improve load distribution and vibration damping, rail infrastructure still suffers from drainage problems, ballast degradation, and subgrade settlement. Water trapped in poorly drained layers reduces bearing capacity, while fouling, cyclic loading, and climate variations accelerate degradation, leading to high maintenance costs [3,4]. To counter these issues, Castro, et al. [5] emphasised that effective waterproofing layers should have residual air voids between 3% and 8% to promote drainage but inhibit moisture ingress; they also found that bituminous sub-ballast layers were more effective than granular layers and that optimum performance was achieved with relatively thin high-modulus hot mix asphalt (HMA) layers. Therefore, developing high-density HMAs capable of withstanding heavy dynamic loads while preventing moisture infiltration remains crucial for high-speed and heavy-haul railways.

Emerging research is exploring sustainable additives and fibres to enhance bitumen performance. Natural fibres (e.g., coir, lignin, bamboo) can improve stiffness and reduce cracking, but dosing must be optimised to avoid excessive air voids. Synthetic fibres such as polyester, polypropylene, and aramid provide chemical resistance and durability. A recent mechanistic study, Cao and Wang [6], found that polyester fibres interspersed into asphalt via aromatic ring interactions, yielding a higher complex shear modulus and lower phase angle than straw fibre-modified asphalt; at 64 °C, the polyester-modified binder showed a phase angle 4.29° lower and exhibited lower creep compliance at low temperatures. Biochar addition has also been shown to increase rotational viscosity and rutting resistance while enhancing fatigue and low-temperature performance [7]. Crumb rubber modification is another sustainable approach: crumb rubber particles swell when blended with asphalt and absorb maltenes, thereby increasing the asphaltene-to-maltene ratio; Sukkari, et al. [8] reported that crumb rubber combined with warm-mix additives improves rutting and fatigue resistance while lowering binder viscosity.

Polymer and nanomaterial modifications have been widely investigated. ASA polymer-based modifiers improve fatigue and rutting resistance at optimal dosages, while excessive polymer can reduce performance; nanosilica and other nanomaterials can reduce rutting depth and improve high-temperature rheology, particularly when used alongside polymers [9]. However, differences in oil sources and filler composition can cause compatibility issues, and there is a continuing need for eco-friendly high-viscosity modifiers that can resist oxidation and ultraviolet ageing [10]. These findings suggest that synergistic combinations of fibres, bio-based additives, crumb rubber, polymers, and nanoparticles may offer enhanced rheological and mechanical properties for asphalt track binders.

Accurate assessment of these modified binders requires rigorous rheological testing. Standard protocols such as EN 13702, EN 16659, and FGSV 722 use Dynamic Shear Rheometer (DSR) tests to determine phase angle (δ), complex shear modulus (G*), and dynamic viscosity (η) across a range of temperatures and frequencies [11,12]. Correlations have been established between viscosity and rutting performance: Sybilski [13] found that higher viscosities at 60 °C correlate with improved rutting resistance, while Morea, et al. [14] noted that rutting increases sharply when viscosity falls below 2000 Pa·s. High-viscosity additives can elevate viscosities from 249 to over 2×10^6 Pa·s at 53–71 °C [15]. Multiple Stress Creep Recovery (MSCR) tests further quantify polymer-modified binder performance via percentage elastic recovery (R%) and non-recoverable creep compliance (Jnr). Building on these methodologies, the present study evaluates how multifunctional

additives, organic compounds, and fibre modifiers influence the rheological behaviour of bitumen for railway applications. To clearly position the present work and its novelty with respect to existing studies on bio-additives, fibres, and multifunctional modifiers for bituminous binders, a short comparative synthesis is first required. Previous investigations have made important contributions by demonstrating the potential of individual sustainable additives (e.g., biochar, crumb rubber, fibres) or limited binary systems to enhance specific rheological or chemical properties of asphalt binders. However, these studies are generally constrained by one or more of the following aspects: (i) focus on single-modifier or binary configurations without explicitly addressing multi-component synergy, (ii) limited consideration of railway-oriented hard (HD) binders and their stringent performance requirements, and (iii) partial performance evaluation, often restricted to selected rheological indicators without a systematic interaction-based framework.

Table 1 summarizes the main characteristics of selected key references and highlights how the present study advances beyond them, particularly in terms of modifier configuration (systematic comparison of single, binary, and ternary blends), interaction analysis (explicit identification of synergistic effects rather than additive responses), and performance evaluation (combined use of DSR temperature sweeps, MSCR parameters, and FTIR analysis to link macroscopic rheology with chemical changes). By adopting a waste-derived ternary system (OC + MA + MFA) and a railway-specific experimental perspective, the present work extends existing knowledge toward a more integrated and application-oriented understanding of modified binders for waterproofing and sub-ballast layers.

Table 1. Positioning of the present study relative to key literature on bio-based and multifunctional asphalt modifiers.

Reference	Modifier System	Waste-Derived	Includes Ternary Interaction	MSCR (R%, Jnr)	FTIR Linked to Rheology	Main Limitation in Prior Work	Advance in This Paper
Xiao, Cai, Lou, Shi and Xiao [4]	Review	-	-	-	-	Review/no factorial interaction	Experimental quantification + interaction effects
Cao and Wang [6]	Fibre/polymer interactions	Partial	-	Sometimes	Sometimes	Not railway HD + not ternary	Railway-oriented HD + full interaction matrix
Martinez-Toledo, Valdes-Vidal, Calabi-Floody, Gonzalez and Reyes-Ortiz [7].	Biochar	Yes	-	Sometimes	Sometimes	Single additive	Adds ternary synergy + MSCR + FTIR link
Sukkari, Al-Khateeb, Zeiada and Ezzat [8]	CR + WMA	Partial	Binary only	Yes	Yes	No fibres/ternary	Extends to ternary incl. fibres + ranking

Thus, the valorisation of modified bitumen systems in railway infrastructure is a key step toward mitigating the challenges posed by rising axle loads and changing conditions. This study integrates an organic compound (OC), multifunctional additive (MA), and modified filamentous additive (MFA) with advanced rheological characterisation to engineer durable, high-performance bituminous systems for waterproofing and sub-ballast applications. Simultaneously, research on incorporating waste-derived modifiers promotes sustainability alongside mechanical resilience. Addressing existing gaps in understanding long-term performance, bitumen ballast interaction, and environmental impacts will advance the design of reliable, low-maintenance railway systems.

The primary objective of this study was to evaluate the rheological properties of bitumen modified with OC, MA, and MFA valorisation of organic-based waste additive materials for potential application in asphaltic waterproofing layers used in railway tracks. Figure 1 shows the experimental design flowchart for this study.

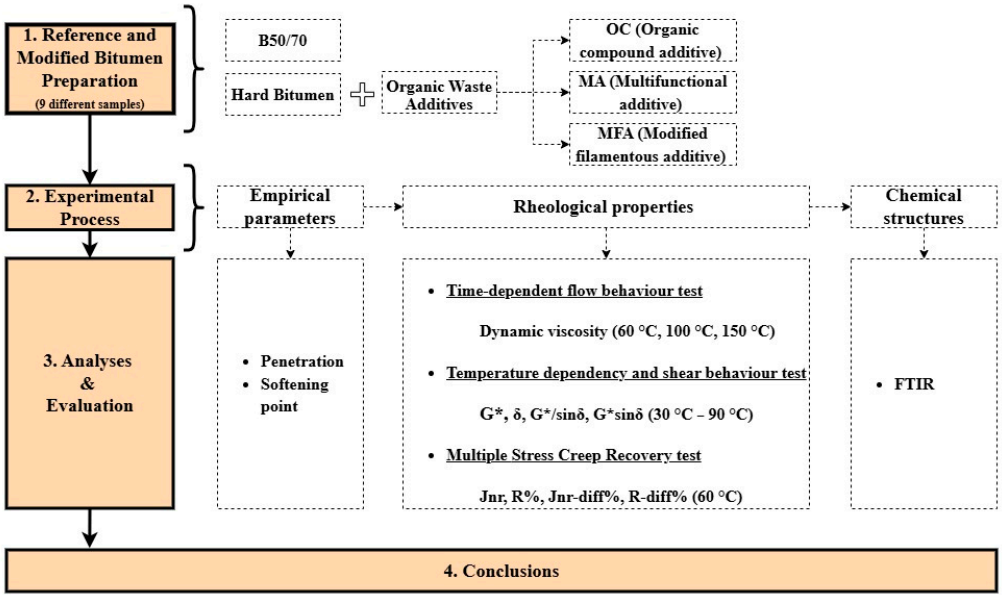

Figure 1. The experimental design flowchart of this study.

To achieve this objective, the research proceeded through the following stages:

- Comprehensive literature review—a survey of existing research on modified bitumen and fibre-reinforced binders (see Section 1).
- Experimental design and testing—selection of materials, preparation of modified binders, and execution of rheological tests (see Section 2).
- Data analysis and interpretation—analysis of rheological test results and formulation of key conclusions (see Sections 3 and 4).

This work provides binder-level performance indicators relevant to waterproofing/sub-ballast applications; however, track-level performance depends on mixture composition, ageing, and structural interaction with ballast and subgrade and is therefore outside the scope of the present experimental program.

2. Materials and Methods

2.1. Raw Materials

Two bitumen types were used: 50/70 penetration-grade from Perretti Petroli S.P.A. (Puglia, Italy) and HD asphalt binder meeting ANAS (Italy) standards. HD is typical for high-stiffness pavements, while B50/70 served as a reference for rheological comparison. Empirical properties are shown in Table 2.

Table 2. Empirical characteristics of reference bitumen B50/70 and HD.

Properties	pen@25	SP	pen@25, RTFOT	SP, RTFOT	FBP	ER@25
Standard	EN 1426	EN 1427	EN 1426	EN 1427	EN12593	EN13398
Unit	0.1 mm	°C	%	°C	°C	%
B50/70	54	48.7	≥40	≤9	≤−8	-
HD	56	76.1	≥40	≤5	≤−12	≥80

Symbols. pen@25: penetration at 25 °C. SP: softening point. pen@25, RTFOT: penetration at 25 °C after rolling thin film oven test. SP, RTFOT softening point increase after rolling thin film oven test. FBP: Fraass breaking point. ER@25: elastic recovery at 25 °C.

In addition, the HD bitumen was modified at various additive contents based on the evaluation of three different waste materials. Figure 2 presents the additives used in this

study: (A) OC, derived from organic materials, containing nitrogen, carbon, and oxygen. (B) MA, surfactant, based on phosphate esters. (C) MFA, cellulose fibre, obtained from cardboard waste, having a size of 0.2–0.6 mm.

Figure 2. OC, MA, and MFA used in this study.

2.2. Bitumen Modifications

The HD asphalt binder was heated to 160 °C, and additives OC (2%), MA (0.5%), and MFA (3%) by bitumen weight were incorporated. The OC (2%), MA (0.5%), and MFA (3%) dosages were selected based on a prior pre-screening campaign performed within the LIFE SILENT project and the MOST project, in which multiple candidate contents were evaluated based on production process (dispersion during mixing, avoidance of excessive viscosity) and performance prediction based on preliminary knowledge. In the present manuscript, these values are therefore adopted as fixed target dosages to isolate the role of each additive and quantify interaction effects through single, binary, and ternary blends. Homogeneous dispersion was achieved by mixing at 160 °C at 1000 rpm for 15 min. Sample codes and blend details are in Table 3.

Table 3. Sample codes.

No	Samples ID	List of the Tests Carried Out (Including Standards)
1	B	Penetration at 25 °C, 0.1 mm (EN 1426). Softening point, °C (EN 1427). Dynamic viscosity (η, mPa·s) at 60 °C, 100 °C and 150 °C, UNI EN (13702:2018). Complex shear modulus (G*, Pa) and phase angle (δ, °) at 30–90 °C, FGSV 722. Percent elastic recovery (R%), non-recoverable creep compliance (Jnr, kPa^{-1}) at 0.1 kPa and 3.2 kPa, and at 60 °C, and Jnr-diff, EN 16659.
2	HD	
3	HD + 2%OC	
4	HD + 0.5%MA	
5	HD + 3%MFA	
6	HD + 2%OC + 0.5%MA	
7	HD + 2%OC + 3%MFA	
8	HD + 0.5%MA + 3%MFA	
9	HD + 2%OC + 0.5%MA + 3%MFA	

Symbols. B: B50/70 bitumen. HD: hard bitumen. HD + 2%OC: hard bitumen + 2% organic compound additive. HD + 0.5%MA: hard bitumen + 0.5% multifunctional additive. HD + 3%MFA: hard bitumen + 3% modified filamentous additive. HD + 2%OC + 0.5%MA: hard bitumen + 2% organic compound additive + 0.5% multifunctional additive. HD + 2%OC + 3%MFA: hard bitumen + 2% organic compound additive + 3% modified filamentous additive. HD + 0.5%MA + 3%MFA: hard bitumen + 0.5% multifunctional additive + 3% modified filamentous additive. HD + 2%OC + 0.5%MA + 3%MFA: hard bitumen + 2% organic compound additive + 0.5% multifunctional additive + 3% modified filamentous additive.

For penetration at 25 °C, 0.1 mm (EN 1426), this is associated with the softness of the bitumen and the climatic conditions in which it is used. Under common environmental conditions, in Italy, the grade 50/70 is often used.

For softening point, °C (EN 1427), low values are associated with mixture rutting and bleeding. HD bitumen must have a value in the range 70–90 °C, and B50/70 must have a value in the range 45–60 °C.

For dynamic viscosity (η, mPa·s) at 60 °C, 100 °C, and 150 °C, UNI EN (13702:2018), its dependency on temperature is crucial. At high temperatures, it is associated with the

mixing and compaction temperatures that affect the workability of the mixtures. In more detail, for compaction, the viscosity should be 0.28 ± 0.03 Pa·s, while for mixing, it should be 0.17 ± 0.02 Pa·s.

For complex shear modulus (G*, Pa) and phase angle (δ, °), (1) at high temperatures (30–90 °C (4)), FGSV 722, high G*/sinδ (>1 kPa) is needed; (2) at medium temperatures, low G*sinδ (<5000 kPa) is needed. This is associated with high rutting resistance (at high temperatures) and high fatigue resistance (at medium temperatures, after the pressure ageing vessel, PAV, ageing), respectively, according to the elastic response under oscillating loads at given temperatures.

For non-recoverable creep compliance (Jnr, kPa^{-1}) at 0.1 kPa and 3.2 kPa, and at 60 °C, EN 16659, low Jnr at 3.2 kPa at high temperatures (<0.5–4 kPa^{-1}, as a function of traffic level, from extremely heavy to standard) is associated with high rutting resistance under light and heavy traffic at high temperatures. For the corresponding Jnr-diff, low values (lower than 75%) correspond to a low susceptibility to load changes. For the corresponding percent elastic recovery (R%), high values (>30%–45%, as a function of Jnr, cf. FHWA-HIF-11-038) are associated with low rutting.

2.3. Testing Methods and Procedures

Figure 3 presents a three-phase experimental framework evaluating bitumen modified with eco-friendly, waste-derived additives under varying temperatures and traffic conditions. Phase 1 characterises virgin (B50/70, HD) and HD-modified binders via empirical tests. Phase 2 analyses rheological behaviour under controlled conditions, assessing OC, MA, and MFA effects on viscoelastic and thermoplastic properties, with correlations visualised through heat maps. Phase 3 investigates chemical interactions among reference bitumen, modifiers, and blends using FTIR spectroscopy, based on infrared light absorption (700 nm–1 mm) linked to molecular vibrations, identifying functional group changes.

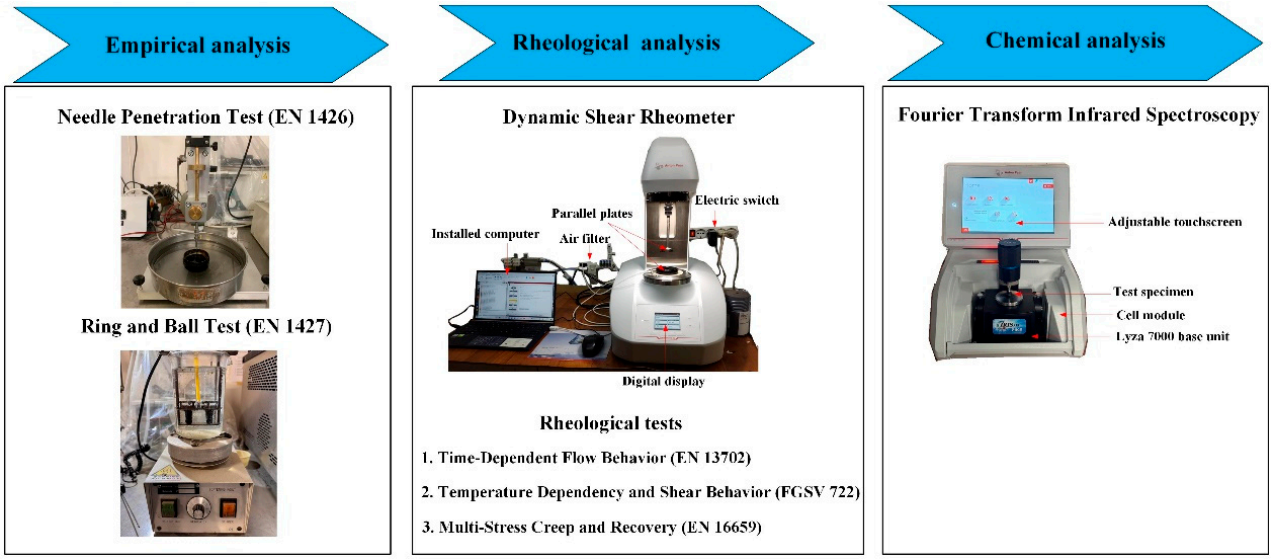

Figure 3. The framework of the experimental study.

2.3.1. Empirical Tests

The basic physical properties of bitumen binders were first evaluated using empirical tests. These included the needle penetration test at 25 °C according to EN 1426 and the softening point test using the Ring and Ball method according to EN 1427 to assess consistency at medium and high service temperatures.

2.3.2. Rheological Analyses

In this study, to determine the rheological properties of reference and modified bitumen, time-dependent flow behaviour tests, temperature-dependent and shear behaviour tests, and MSCR tests were conducted in a laboratory environment using a DSR.

(a) Time-dependent flow behaviour test

The time-dependent flow test, following EN 13702:2018, evaluates viscosity under constant shear and isothermal conditions as a preliminary assessment of material flow at a fixed temperature. Using a DSR SmartPave 92 (Anton Paar) with PP25 plate geometry and 1 mm gap, tests were conducted at 60 °C, 100 °C, and 150 °C. After 10 min of temperature equilibrium, viscosity was measured for 400 s at shear rates of 0.05, 50, and 500 s^{-1}. This approach provides insight into bitumen behaviour under controlled conditions, supporting material optimisation and quality assurance.

(b) Temperature dependency and shear behaviour test

In this case, the modified bitumen samples were prepared in accordance with FGSV 722, which defines the determination of deformation behaviour to remove air, poured into silicone moulds (AASHTO T 315), cooled, and stored for 2 h for virgin and 12 h for polymer-modified bitumen (maximum 36 h). DSR testing used a 25 mm plate geometry with a 1 mm gap, controlled by a Peltier system (±0.1 °C). Temperature sweeps (30–90 °C) followed FGSV 722, within the linear viscoelastic range, using 1.59 Hz oscillation (≈10 rad/s, ≈90 km/h traffic speed). Parameters G* (total resistance to deformation) and δ (viscous response; 0° = elastic, 90° = viscous) were recorded. These procedures ensured reliable, reproducible characterisation of modified bitumen rheology under varying temperatures, aligning with standardised testing protocols.

(c) Multiple Stress Creep Recovery (MSCR) test

MSCR, as defined by EN 16659, was employed to evaluate the viscoelastic behaviour of bituminous binders under repeated loading and unloading cycles, each cycle lasting 10 s. Using a DSR, the test was conducted at 60 °C to determine key parameters: R% (percent recovery) and Jnr (non-recoverable creep compliance).

The R% value is calculated from stresses and shear strains using Equation (1):

$$R_{\sigma}^{N} = \frac{\epsilon_{1}^{N} - \epsilon_{10}^{N}}{\epsilon_{1}^{N}} \times 100 \quad (1)$$

where R_{σ}^{N} is the percentage recovery at the applied stress σ (kPa) after N-th loading cycles, ϵ_{1}^{N} is the shear strain at the first load, and ϵ_{10}^{N} is the shear strain, measured after recovery at the tenth of the N-th cycle. The average percentage recovery at the given stress level is then calculated as follows:

$$R_{\sigma} = \frac{1}{10}\sum_{N=1}^{10} R_{\sigma}^{N} \quad (2)$$

The non-recoverable creep compliance at a given stress is calculated using Equation (3):

$$Jnr_{\sigma}^{N} = \frac{\epsilon_{10}^{N}}{\sigma} \quad (3)$$

where ϵ_{10}^{N} is the non-recoverable strain at the N-th cycle, and σ is the applied stress. The average Jnr at a stress of 0.1 kPa is given by the following:

$$Jnr_{ave} = \frac{1}{10}\sum_{N=1}^{10} J_{nr,\,0.1kPa}^{N} \quad (4)$$

The nonlinearity and elastic recovery of the binders were evaluated using the following parameters:

$$Jnr - diff = \frac{Jnr_{@3.2\text{kPa}} - Jnr_{@0.1\text{kPa}}}{Jnr_{@3.2kPa}} \times 100 \quad (5)$$

$$R - diff = \frac{R_{@0.1\text{kPa}} - R_{@3.2\text{kPa}}}{R_{@0.1\text{kPa}}} \times 100 \quad (6)$$

where $Jnr - diff$ is the percentage difference in Jnr between stress levels of 0.1 kPa and 3.2 kPa, indicating the nonlinearity of the binder, and $R - diff$ represents the binder's ability to retain elastic behaviour between these stress levels. These parameters quantify the elastic recovery and the susceptibility to permanent deformation, respectively, under controlled stress levels. Consequently, they pertain to the resistance to plastic deformation. Lower Jnr corresponds to higher rutting resistance and vice versa. Consequently, the aim is to have lower Jnr requirements when heavy traffic is expected (e.g., 1–2 kPa^{-1} instead of 4.5 kPa^{-1} [16]. The supplementary requirement is that the Jnr-diff should not be greater than 75%. The R-diff% quantifies the drop in elastic recovery between low and high stress levels (R%@0.1kPa vs. R%@3.2kPa) and thus serves as an indicator of stress-sensitivity in the binder's recovery behaviour. A high R-diff% value implies a large loss of recoverability under increased stress (i.e., the binder is less able to "spring back" when subjected to heavier loads), which may signal a reduced resistance to permanent deformation. Jnr-diff refers to non-recoverable strains and R-diff to elastic strains. For both, the higher the Jnr-diff and R-diff is, the greater the sensitivity to changes in stress levels.

2.3.3. Chemical Analyses: FTIR

FTIR analysis using multiple reflection ATR (Anton Paar Lyza 7000, Anton Paar, Ashland Graz, Austria) was conducted to characterise the functional groups of B50/70, HD, and HD modified with OC, MA, and MFA. Pure and modified bitumen samples were dissolved in cyclohexane at a 1:3 (bitumen: cyclohexane) ratio and left for 24 h. A 0.1 mL aliquot was placed on the crystal, and after solvent evaporation, a 35 µm film was formed for FTIR examination. Each sample underwent three measurements with 32 scans in the 400–4000 cm^{-1} range and 1.33 cm^{-1} resolution. Transmission spectra were converted to absorbance spectra, focusing on the 2500–3600 and 690–1800 cm^{-1} ranges. According to the literature [17,18], main detectable components include (1) hydrocarbons (CH_2, CH_3) at 2850–2920 and 1380–1600 cm^{-1}; (2) carbonyls (1655–1730 cm^{-1}); (3) aromatics (~1600 cm^{-1}); (4) sulfoxides (1030–1260 cm^{-1}); and (5) polyaromatics (<1000 cm^{-1}). These components are key indicators of reclaimed asphalt pavement content and bitumen ageing. Functional group wavelength ranges for B50/70 are presented in Table 4 and referenced in subsequent analyses.

Table 4. Functional groups in bitumen.

Wavenumber cm^{-1}	Functional Group	Vibration	Type
720	Alkyls	γ (CH_{2n})	Hydrocarbon
750	Aromatic	γ CH_{aro}	Hydrocarbon
810	Sulphate Ester	ν S–O–C	SCC
870	Aromatic	γ CH_{aro}	Hydrocarbon
910	Alkene	δ (CH)	Hydrocarbon
1030	Sulfoxides	ν S=O	SCC
1060	Sulfones	ν SO_2 (in-phase)	SCC
1120	Sulphate ester	ν_{as} SO_2 (out-of-phase)	SCC
1260	Sulphate ester	ν_{as} SO_3	SCC
1380	Alkyls	δ_{as} CH_2/CH_3	Hydrocarbon

Table 4. *Cont.*

Wavenumber cm^{-1}	Functional Group	Vibration	Type
1455	Alkyls	δ_{as} CH_2/CH_3	Hydrocarbon
1600	Aromatic	ν C=C_{aro}	Hydrocarbon
1655	2-Quinoline	ν C=C	Carbonyl
1700	Ketone	ν C=O	Carbonyl
1730	Carboxylic acids	ν C=O	Carbonyl
2850	Alkyls	ν_{as} CH_2/CH_3	Hydrocarbon
2920	Alkyls	ν_{as} CH_2/CH_3	Hydrocarbon

Note ν: stretching vibration; ν_{as}: asymmetric stretching; γ: out-of-plane bending; δ: in-plane bending; δ_{as}: asymmetric bending; SCC: sulphur-containing compound.

3. Results and Discussion

3.1. Empirical Test Results

According to the empirical test results in Figure 4, although the softness of HD bitumen is similar to B50/70 bitumen, the temperature required to transition from a solid or semi-solid state to a viscous state is 67% higher. Indeed, it should be noted that the softening point of hard bitumen exceeds 80 °C. This situation should be considered because of the temperatures (60–80 °C) of common tests (DSR, MSCR, etc.) used to determine rheological properties. Moreover, an examination of the average difference results (Figure 4c) for modified HD binders relative to HD bitumen shows that all additives reduce penetration values while increasing softening points. Among the additives, MFA demonstrated the most significant influence on penetration and softening points, whereas OC exhibited the least effect.

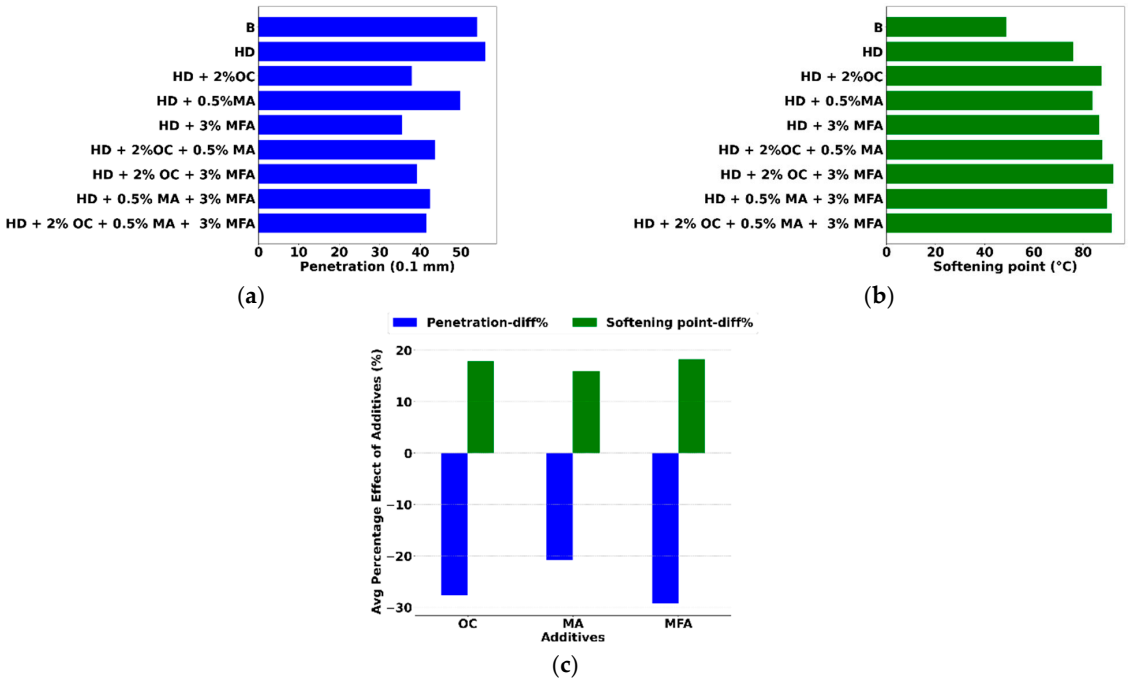

Figure 4. Empirical test results for reference and modified bitumen, (**a**) penetration, (**b**) softening point, and (**c**) average effect of additives in percentage.

3.2. Time-Dependent Flow Behaviour

The results of the time-dependent flow behaviour test are shown in Figure 5. The obtained viscosity results highlighted the difference in the flow behaviour of modified HD asphalt binders (with OC, MF, and MFA) at different temperatures compared to the reference HD asphalt binder. With respect to HD, for HD + 2%OC, the viscosity slightly

decreased at 150 °C but increased at 100 °C and at 60 °C. This indicated that OC improved the flow ability of bitumen at elevated temperatures, which is consistent with the findings of Dyuryagina, et al. [19] and Li, et al. [20]. It should be emphasised that this refers to the OC-only blend (HD + OC), while combined blends (including also OC but not only OC) do not necessarily preserve the reduction observed for OC alone. In the case of HD + 0.5%MA, a slight decrease in viscosity was observed at 150 °C (−5.03%), with only minor variations at lower temperatures. MA appeared to enhance the elasticity of bitumen, particularly at higher temperatures, as reported by Fazaeli, et al. [21] and Remisova, et al. [22]. The addition of 3% MFA (HD + 3%MFA) resulted in a substantial increase in viscosity across all temperatures, with the most pronounced effect at 100 °C (32.41%). This behaviour was attributed to the formation of a structural network within the bitumen by MFA, which increased stiffness and thickness, as supported by Mirsephahi, et al. [23]. The HD + 2%OC + 0.5%MA blend exhibited the most significant viscosity increase at 150 °C, suggesting that the two additives acted synergistically to improve the strength and thermal stability of the bitumen, in agreement with Dyuryagina, Byzova, Ostrovnoy, Demyanenko, Tyukanko and Lutsenko [19] and Li, Liu, Xiao, Li, Wang and Peng [20].

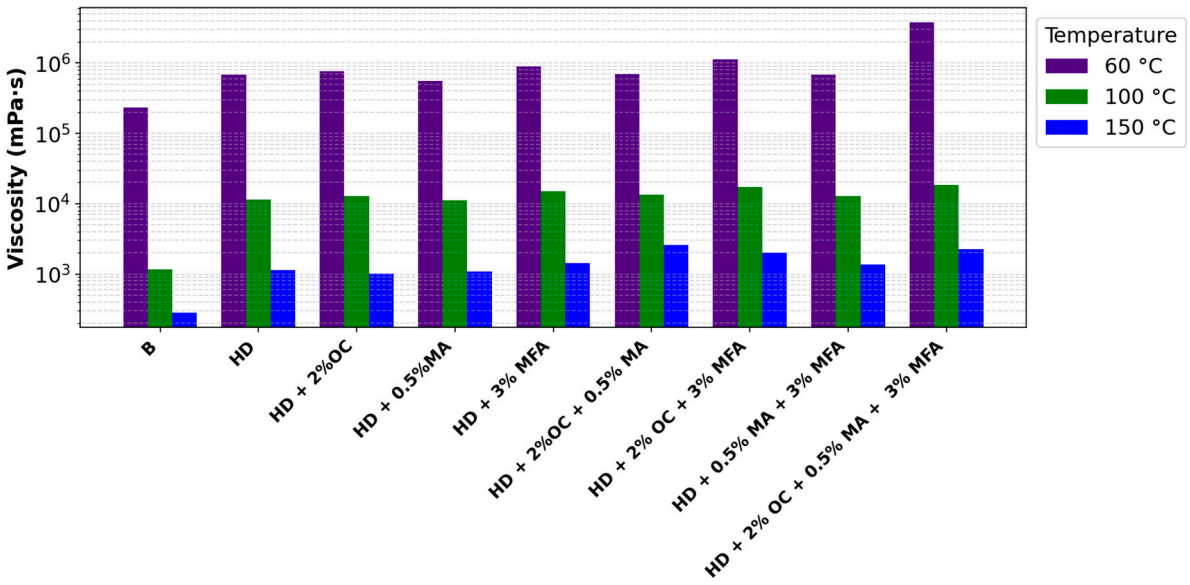

Figure 5. Dynamic viscosity (η) of the HD asphalt binders under different temperature conditions (60 °C, 100 °C, 150 °C).

The mixing and compaction temperatures required for producing asphalt mixtures with reference and modified asphalt binders increase as the rate of decrease in viscosity with rising temperature (Table 5). Consequently, modified bitumen (such as HD + 2%OC + 0.5%MA, which exhibits the highest viscosity at 150 °C) requires significantly higher mixing and compaction temperatures compared to the other binders. In contrast, the HD + 2%OC binder needs lower temperatures due to its relatively lower viscosity at the same test temperature. This finding can indicate that the OC additive improves workability. However, the inclusion of modifiers such as MFA enhances the stability of the mixture, though MFA-modified HD binders can require higher temperatures to achieve sufficient fluidity and ensure effective mixing with aggregates. Importantly, it is noted that a viscosity reduction can also be obtained through different mechanisms that are not easily detected through bitumen-related analyses (surfactants, working at the micro-scale between bitumen and aggregates). These results are consistent with empirical test results of MFA-modified HD binders, which revealed increased hardness (lowest penetration and

highest softening point). To support this study, it is noted that while Rodríguez-Alloza and Gallego [24] emphasised the reduction in mixing and compaction temperatures with the addition of the organic additives, Crispino, et al. [25] reported that cellulose-based fibres increased the required temperatures.

Table 5. Mixing and compaction temperatures of asphalt mixtures with different additive.

Sample	T Compaction (°C)	T Mixing (°C)
B	147	158
HD	170	184
HD + 2%OC	168	181
HD + 0.5%MA	169	183
HD + 3%MFA	174	188
HD + 2%OC + 0.5%MA	185	201
HD + 2%OC + 3%MFA	181	196
HD + 0.5%MA + 3%MFA	173	187
HD + 2%OC + 0.5%MA + 3%MFA	184	199

In general, the higher mixing and compaction temperatures required for both reference and modified HD bitumen, compared to B, may require greater energy and temperature control in mixing plants and on-road applications. This increases fuel consumption and costs, as well as CO_2 emissions. Furthermore, insufficient fluidity makes bitumen difficult to pump or spray. High hardness can also hinder adequate adhesion to aggregate. Furthermore, a hard binder can increase the risk of cracking at low temperatures. However, it does increase rutting resistance, but this advantage must be balanced against application challenges. Against these observations, it is important to highlight that the tests above do not offer the possibility to come to conclusions in terms of adhesion but mostly focus on cohesion.

3.3. Temperature Dependency and Shear Behaviour Test

Temperature dependence and shear behaviour testing is performed using a DSR to investigate the elastic response under oscillating loads at high (30–90 °C) service temperatures. The parameters (G*, δ) obtained from oscillation test results are given in Figure 6. According to Figure 6, the reference HD asphalt binder exhibited much higher G* values than B50/70 bitumen at elevated temperatures, reflecting its inherent characteristics as a hard binder commonly used in road pavements requiring strength and rutting resistance. However, temperature effects significantly influenced this behaviour, with higher temperatures facilitating molecular mobility and amplifying the reduction in G*. This was consistent with rheological models showing shear thinning (where the viscosity decreases under shear strain) for high temperatures [12,26]. In addition, its rutting resistance diminished at higher temperatures, as evidenced by the rising δ values with increasing temperature. As an interesting finding, it should be noted that only δ values of the reference B50/70 and HD asphalt binders increased with increasing temperature after 40 °C, while the phase angle of all modified bitumen decreased. In modified binders, the polymer network or crosslinking may become more dominant at higher temperatures, resisting viscous flow and thus making the behaviour more elastic (lower δ). Some modified binders show a bimodal δ trend (increase then decrease) at high temperatures [27–30]. Among the modified bitumen, HD + 3%MFA showed the highest G* values across the 30–90 °C range, clearly indicating better stiffness and rutting resistance, while its phase angle changed only slightly with temperature increase. This demonstrated that MFA effectively enhanced binder performance by reducing bitumen viscosity even under high temperatures, thereby improving resistance to deformation. These findings corroborated prior work on modified

asphalt rheology, which noted improved flexibility and delayed structural breakdown due to material composition [31,32]. Moreover, δ analysis showed that samples with higher OC content had lower δ values, signifying enhanced elasticity at elevated temperatures.

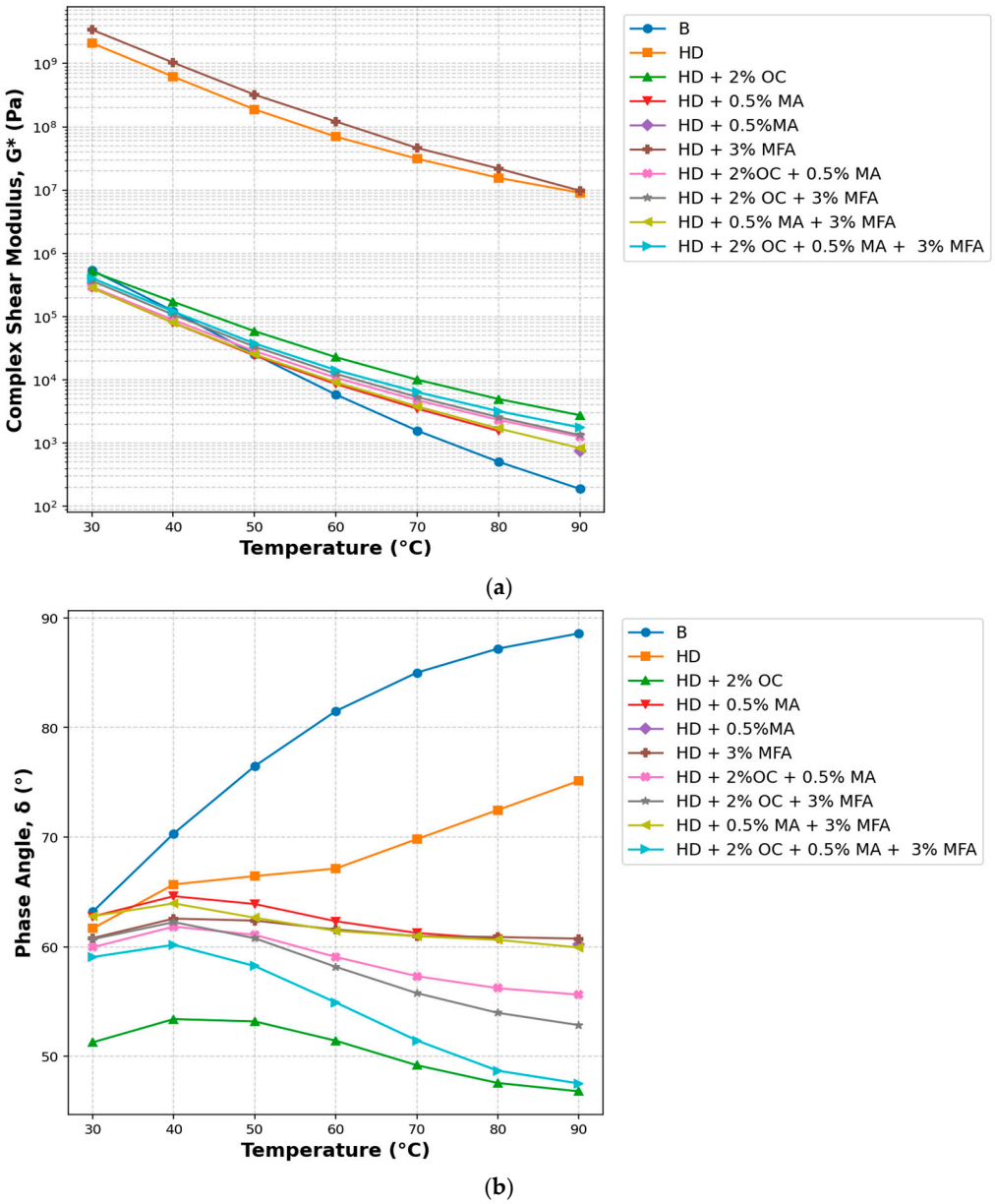

Figure 6. Temperature dependency and shear behaviour test results: (**a**) complex moduli, G*; (**b**) phase angel, δ.

The results of the rutting (G*/sin δ) resistance parameters showed in Figure 7 that all HD bitumen exhibited significantly higher resistance (at least 10^6 times) than B50/70 bitumen across all temperatures. Among the modified samples, the HD + 3%MFA blend demonstrated the greatest improvement, with rutting resistance value 60.69% higher than reference HD bitumen. This indicates that HD + 3%MFA provides the highest overall resistance, achieving a favourable elasticity and stiffness, particularly under high-temperature and heavy-traffic conditions. However, it is noteworthy that the G* values of HD bitumens are quite higher than that of B50/70 bitumen, causing these bituminous blends to behave more brittle and thus reducing fatigue cracking resistance. As seen in Figure 8, fatigue cracking resistance (G*sinδ values) decreased with increasing temperature for all asphalt

binders, and B50/70 bitumen showed the best performance, followed by HD + 0.5%MA and HD + 0.5%MA + 3%MFA.

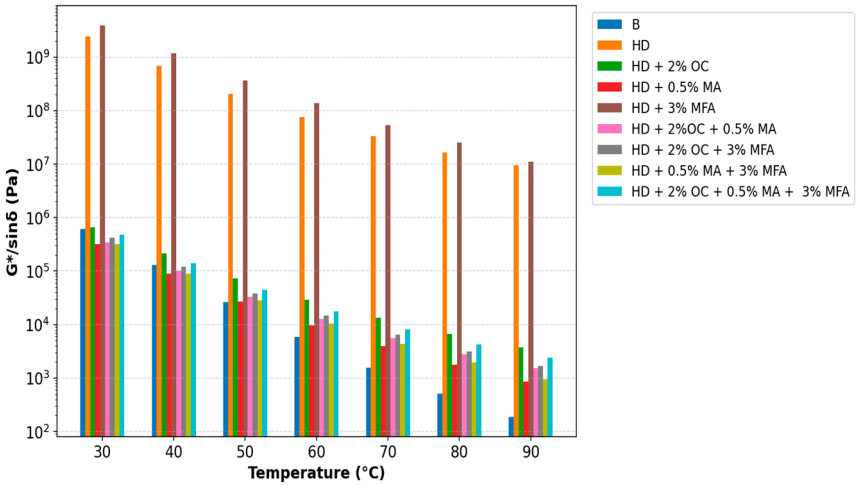

Figure 7. Rutting resistance parameter (G*/sinδ) of the samples.

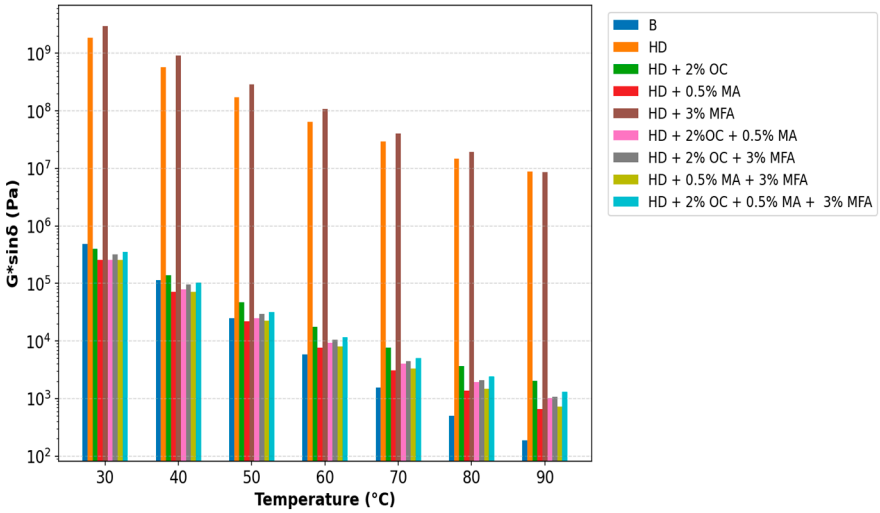

Figure 8. Fatigue cracking resistance parameters (G*sinδ) of the samples.

Figure 9 shows the average difference (%) in rutting and fatigue cracking resistance of each asphalt binder with temperature change (from 30 to 90 °C). Notably, the inclusion of OC lowered temperature sensitivity; for example, the HD + 2%OC blend exhibited the smallest change in rutting and fatigue resistance with increasing temperature. Furthermore, as the temperature increased from 30 °C to 90 °C, the average reduction in rutting resistance observed with each additive separately (60.22%) was less pronounced (57.38%) in the sample containing all three additives. Consequently, the HD + 2%OC + 0.5%MA + 3%MFA blend provided a more balanced temperature-dependent performance, combining elasticity and stiffness in a way that enhanced both rutting resistances. These findings are consistent with prior research. Li, Liu, Xiao, Li, Wang and Peng [20] and Erkuş, et al. [33] emphasised the role of organic and multifunctional additives, as well as fibres, in enhancing the rheological performance, stiffness, and elasticity of bitumen. Similarly, Rodríguez-Alloza, et al. [34] reported that organic additives improve softening points and penetration resistance, while Xiao, Cai, Lou, Shi and Xiao [4] highlighted the contribution of fibres to mechanical property enhancement under heavy-load conditions. However, although it was determined that B50/70 bitumen showed a superior performance in fatigue resistance, the effect of HD

bitumen and OC, MA, and MFA additives on fatigue resistance decreased by 16.96% with increasing temperature.

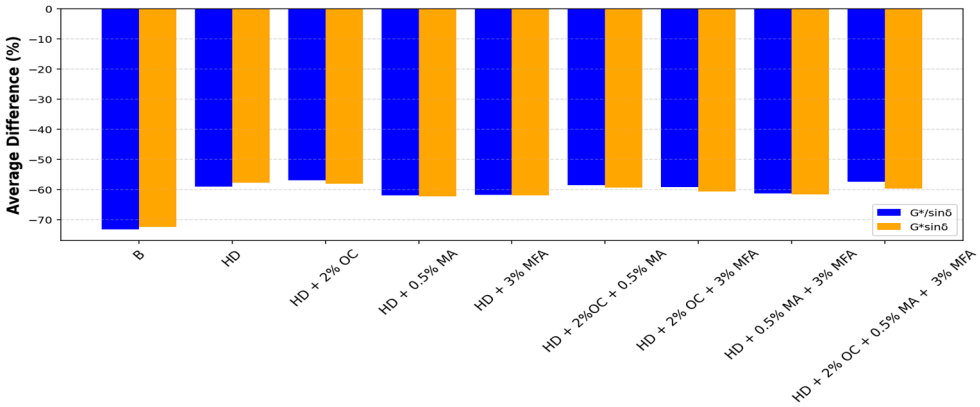

Figure 9. Average difference (%) in rutting and fatigue cracking resistance of each asphalt binder with temperature change.

3.4. MSCR Test Results

Figure 10 illustrates the time-dependent shear strain behaviour of HD asphalt binders under MSCR testing. The results demonstrated significant differences in shear strain accumulation and recovery characteristics between the reference asphalt binders. Over time, the highest shear strain values reached up to 52% in reference B50/70 bitumen, whereas in reference HD asphalt binder, this value did not exceed 15%. This result confirms that HD bitumen is less susceptible to permanent deformation under cyclic loading compared to B50/70 bitumen. However, the absence of additives in reference HD asphalt binder resulted in limited structural support and a reduced ability to effectively resist creep deformation. As reported by Porot, et al. [35], unmodified bitumen lacked polymeric or chemical modifications that enhance elasticity and improve resistance to rutting at elevated temperatures.

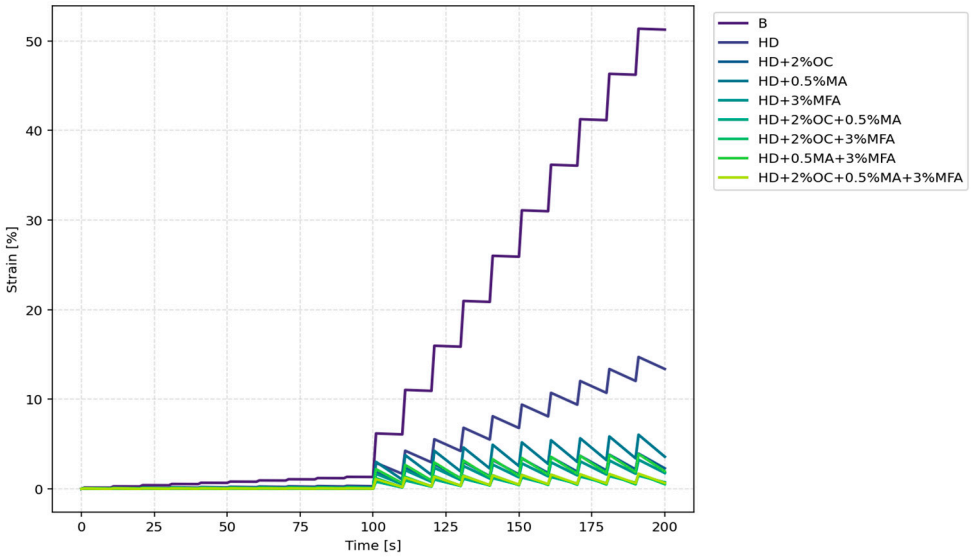

Figure 10. Time-dependent shear strain behaviour of base and modified HD asphalt binders.

The incorporation of additives significantly improved the performance of HD asphalt binders by reducing shear strain, although the extent of improvement varied with the type of additive. OC and MFA demonstrated the most notable effects, lowering strain to approximately 4% and 3.25%, respectively, thereby providing superior resistance to

permanent deformation through enhanced stiffness and elasticity [35–37]. MA modification yielded a moderate reduction in strain (≈6%), functioning primarily as a modifier that increased stiffness while maintaining partial elastic recovery [38]. Overall, MFA and OC exhibited comparable levels of improvement, whereas MA showed less pronounced but still beneficial effects. The results clearly demonstrated that among the modified HD asphalt binders, the ternary additive-modified binder (HD + 0.5%MA + 2%OC + 3%MFA) exhibited the best performance, with a shear strain value below 1.7%. This outcome highlighted the cumulative effect of the additives in enhancing both stiffness and elastic recovery. Such performance rendered this binder highly suitable for applications demanding best rutting resistance under high stress and elevated temperature conditions. These findings align with the existing literature. Organic additives, as demonstrated by Alisov, et al. [39], improve elasticity by forming a viscoelastic network. Similarly, MFA enhances stiffness, as noted by Porot, Zhu, Wang and Cannone Falchetto [35], who emphasized the superior rutting resistance of modified binders. Multifunctional additives, according to Habbouche, Hajj, Sebaaly and Piratheepan [38], strike a balance between elasticity and stiffness, making them critical for high-performance applications. The synergistic effect of using OC, MFA, and MA together further confirmed the findings of Sybilski [13], who highlighted the significant improvements achieved by integrating multiple modifiers.

Figure 11 shows the comparison of R% and Jnr values at 0.1 kPa and 3.2 kPa stress levels for modified HD asphalt binders. The reference HD asphalt binder exhibited weak elasticity (R%: 60.81 at 0.1 kPa; 49.97 at 3.2 kPa) and poor resistance to permanent deformation (Jnr: 0.2891 and 0.4043). The addition of 2% OC significantly improved elasticity, increasing R% to 85.71 and 88.85 while reducing Jnr by 72%–84%. A similar trend was observed with 3% MFA, which achieved slightly higher elasticity (R% ≈ 88.7 at both stress levels) and stronger Jnr reductions (≈82%–85%). This shows that both modifiers alone contribute markedly, with MFA being marginally more effective in reducing Jnr and OC slightly stronger in elasticity recovery. When combined (2%OC + 3%MFA), the improvements were far greater than with individual additives: R% values reached 94.9 and 95.54, reflecting synergistic elasticity gains of 56% and 91% over reference HD. Meanwhile, Jnr dropped even further, and the best performance was obtained with samples containing all additives (HD + 0.5%MA + 2%OC + 3%MFA), yielding the lowest Jnr values (0.019 and 0.02), corresponding to >93% reduction.

Hard, low-penetration/high-softening-point modified HD binders exhibited anomalous MSCR behaviours upon testing in two viscoelastic regimes (0.1 kPa and 3.2 kPa). It should be pointed out that certain studies report constraints in using the Jnr-diff parameter in the MSCR test, particularly for hard binders with very low Jnr values at both 0.1 kPa and 3.2 kPa, where Jnr-diff values may be extremely low or even negative [40–42]. In this case, nonlinear viscoelastic response, stress sensitivity changes of the microstructure/network, and elastic mechanisms that are stress- and binder chemistry-dependent (e.g., entropy-type and energy-type elasticity) may have caused Jnr and R to respond in opposing directions with increasing stress [43–45]. The 0.1 kPa stage exercises linear (or nearly linear) viscous-dominated response, 3.2 kPa forcing the binder into an elastic energy storage-dominated nonlinear regime in which several relaxation paths dominate [46]. This stress dependence is the key objective of the MSCR methodology and the reason that parameters can reverse direction with stress [47,48]. That is, the MSCR protocol applies a low stress and subsequently a higher stress to the material to reveal stress-dependent nonlinear behaviour. Certain binders, therefore, show unusual Jnr or R trends across these levels, e.g., negative percent differences when the high-stress response is more elastic or less compliant than the low-stress response, contrary to the usual expectation that Jnr increases with stress and R decreases with stress [29]. Recent comparative literature reports at least two elastic

contributions: a form of entropy elasticity (recoverable network behaviour) and a form of energy elasticity (stiffer, perhaps brittle response) [49]. Their relative magnitudes can vary with stress or composition such that compliance or recovery may react non-monotonically across stress levels [50]. A stiff modified binder may contain rigid fractions or transient networks that are relatively inactive at very small applied stress but become engaged under higher applied stress, producing more instantaneous elastic recovery and thus lower determined Jnr at 3.2 kPa than measured at 0.1 kPa in some cases [37,40]. Therefore, their Jnr vs. stress curves are not monotonically decreasing. Some materials exhibit lower Jnr at one stress level while deteriorating at another, as network integrity can be a function of stress amplitude [51].

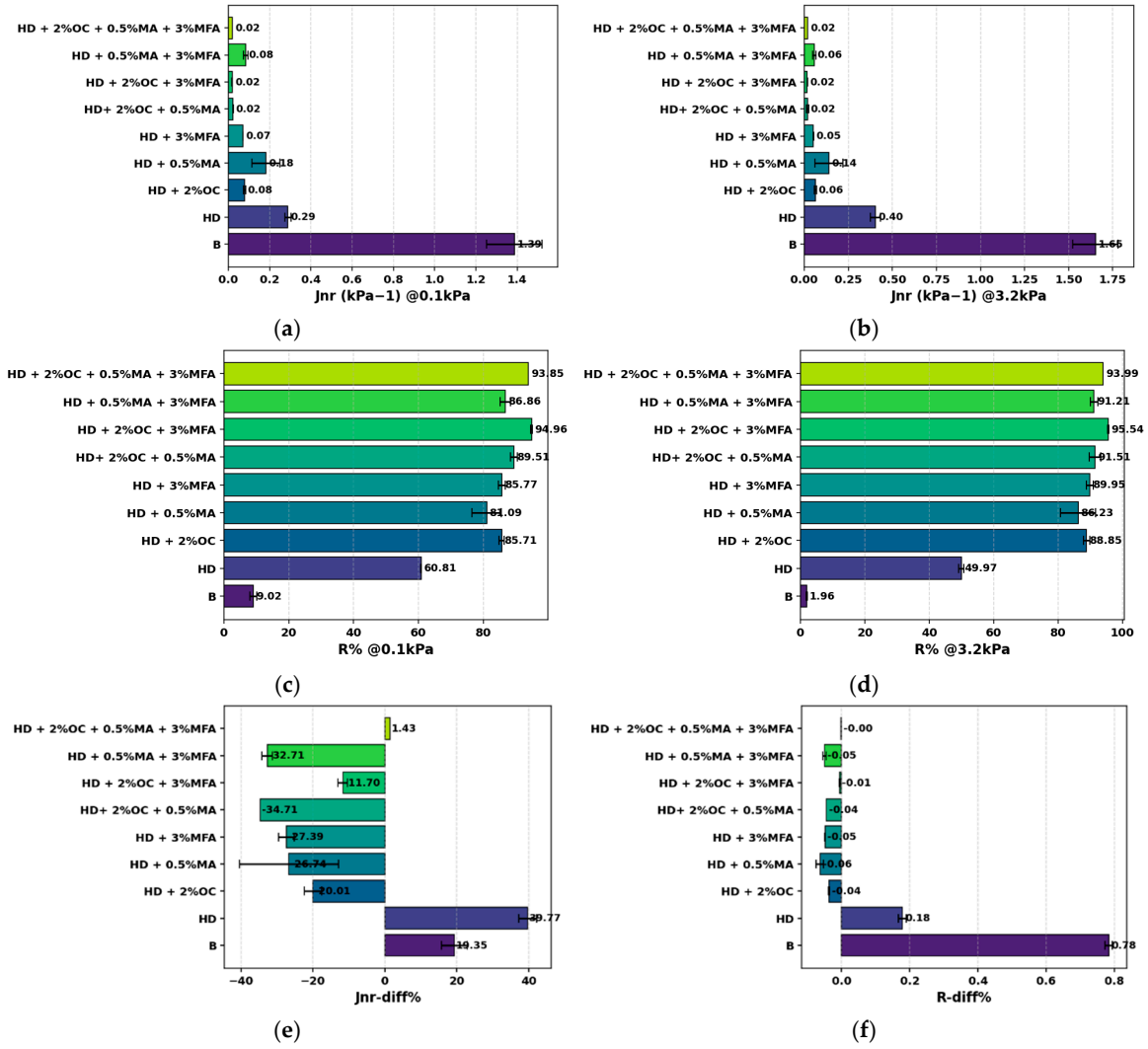

Figure 11. Comparison of R% and Jnr values at different stress levels (0.1 kPa and 3.2 kPa) for modified HD asphalt binders: (**a**) Jnr at 0.1 kPa; (**b**) Jnr at 3.2 kPa; (**c**) R% at 0.1 kPa; (**d**) R% at 3.2 kPa; (**e**) Jnr-diff%; and (**f**) R-diff%.

3.5. FTIR Test Results

Figure 12 and Table 6 show the FTIR analysis results of the reference and modified bitumen, where FTIR plots graphically illustrate the (chemical bond) absorbance (of specific frequencies of infrared light) as a function of the wavenumber (reciprocal of the wavelength absorbed), with emphasis on the three main areas considered. At the same time, Table 6 reports the relative quantification of these areas.

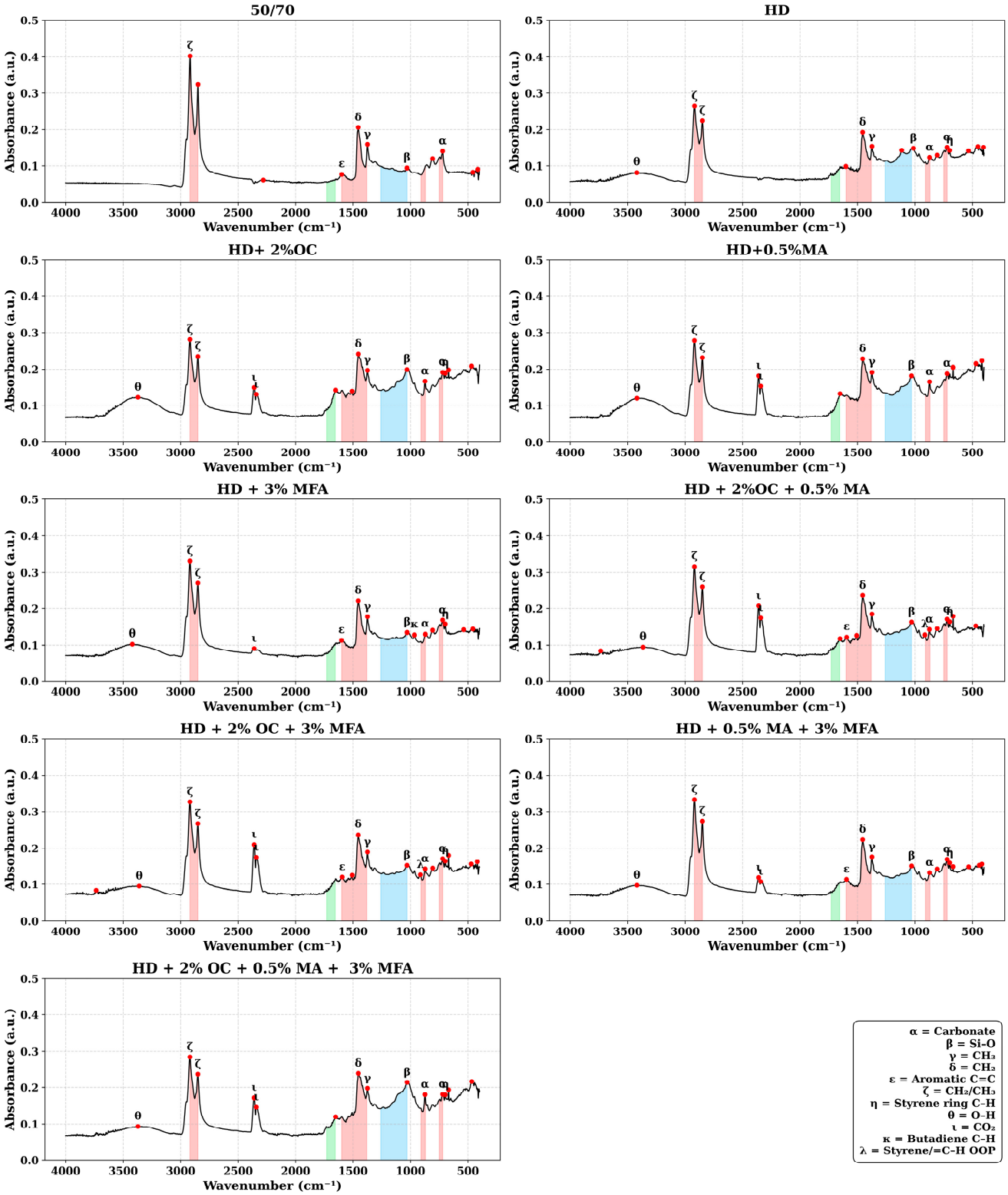

Figure 12. FTIR analysis results.

By referring to FTIR-related analyses, it is important to highlight that three analyses were carried out in this study: (A) comparing the HD spectrum with other spectra (Section 3.5.1), (B) comparing the HD spectrum with the B50/70 spectrum (Section 3.5.2), and (C) analysis of the Pearson coefficients between areas and percentage of single components (Section 3.7).

Table 6. Area absorbance × wavenumber in the FTIR plot.

Specimen (Blend)	Hydrocarbon Area (Rose, 870, 910, 1380–1600, 2850–2920 cm^{-1})	Carbonyl Area (Green, 1655–1730 cm^{-1})	Sulphur Area (Bleu, 1030–1120 cm^{-1})
50/70	46.01	4.32	20.73
HD	47.09	5.96	28.36
HD + 2%OC	60.12	7.88	36.15
HD + 0.5%MA	56.98	7.25	33.08
HD + 3%MFA	53.14	6.45	27.39
HD + 2%OC + 0.5%MA	56.78	7.19	31.54
HD + 2%OC + 3%MFA	56.97	6.91	30.25
HD + 0.5%MA + 3%MFA	53.60	6.53	28.79
HD + 2%OC + 0.5%MA + 3%MFA	58.92	7.20	38.12

Note. Areas have the units of measure of a.u. × wavenumber, where a.u. stands for arbitrary unit, and wavenumbers are expressed in cm^{-1}.

In the first analysis, the HD spectrum is used as the baseline to quantify changes induced by the additives. On the contrary, the second analysis compares the reference 50/70 binder against HD to highlight differences between base binders. In the analyses above, for each spectrum, several metrics were used to quantify similarity or difference. The metrics are defined as follows:

1. Root-mean-squared deviation (RMSD)—Measures the typical size of the deviations between two spectra. It is the square root of the mean of the squared differences:

$$RMSD = \sqrt{\frac{1}{N}\sum_{i=1}^{N}(s_i - r_i)^2} \quad (7)$$

This Equation (6) corresponds to the standard definition of RMSD used for spectral data.

2. Mean absolute deviation (MAD)—Computes the average magnitude of the differences without squaring, making it less sensitive to outliers. It is given by Equation (8).

$$MAD = \frac{1}{N}\sum_{i=1}^{N}|s_i - r_i| \quad (8)$$

3. Pearson correlation coefficient (Corr)—Evaluates the similarity in spectral shape, independent of absolute intensity. It is the normalized covariance between the demeaned spectra:

$$\text{Corr} = \frac{\sum_{i=1}^{N}(s_i - s_{mean})(r_i - r_{mean})}{\sqrt{\sum_{i=1}^{N}(s_i - s_{mean})^2}\sqrt{\sum_{i=1}^{N}(r_i - r_{mean})^2}} \quad (9)$$

where s_i denotes the absorbance at the i-th wavenumber for the sample spectrum, and r_i represents the absorbance at the corresponding wavenumber of the reference spectrum. Both spectra are sampled at N identical wavenumber points; s_{mean} and r_{mean} are the mean absorbance values of the sample and reference spectra, respectively.

It may be observed that high values of RMSD or MAD correspond to high differences between the FTIR areas of the concerned couple of blends (e.g., HD vs. B50/70). On the contrary, high absolute values of the correlation coefficient correspond to a strong linear relationship between the concerned couple of blends. In other terms, higher values of RMSD and MAD indicate larger overall differences, while correlation coefficient (corr) quantifies the similarity of the overall spectral shapes (1 = identical); for integrated area under the absolute absorbance curve (computed by trapezoidal integration), a larger area

reflects a greater total absorbance and hence more or stronger polar functional groups; and for number of prominent peaks identified via peak-finding (prominence threshold 0.02), a higher count implies a more complex spectrum.

3.5.1. Analysis Relative to HD

In this analysis, the HD spectrum served as the baseline. Table 7 summaries the deviation metrics for each modified sample relative to HD. Integrated area values for the absolute absorbance of each spectrum are also included for context. All modified binders have larger integrated areas than HD (334.58 AU·cm^{-1}). The largest increase (around 27%) is observed for HD + 2%OC, implying the OC additive introduces numerous polar functional groups or enhances existing absorbance. MFA yields a modest area increase, whereas MA contributes strongly when combined with OC or MFA. The number of significant peaks increases slightly with additives, reflecting new vibrational modes. The combination of OC with MA and MFA produces the most peaks, indicating overlapping contributions from sulphur- and silica-containing groups.

Table 7. Deviation metrics of modified binders relative to HD.

Sample	RMSD vs. HD	MAD vs. HD	Corr vs. HD	Area (AU·cm^{-1})	Peaks	Key Observations
HD + 2%OC	0.031	0.025	0.94	425.43	15	Largest increase in area; new peak near 1030 cm^{-1} (sulfoxide) and low-wavenumber Si–O–Si bands.
HD + 0.5%MA	0.028	0.022	0.93	413.77	14	Additional carbonyl peaks near 1695–1730 cm^{-1} due to MA.
HD + 3%MFA	0.014	0.012	0.97	371.92	15	Highest correlation with HD; mainly intensifies existing peaks; area increases modestly.
HD + 2%OC + 0.5%MA	0.022	0.017	0.94	395.40	19	Exhibits both sulfoxide (1030 cm^{-1}) and carbonyl peaks; increases low-wavenumber peaks due to fillers.
HD + 2%OC + 3%MFA	0.022	0.016	0.93	392.15	19	Similar to above but with more peaks; suggests overlapping contributions from fillers and OC.
HD + 0.5%MA + 3%MFA	0.015	0.012	0.98	375.97	17	Slight increase in area and peaks; spectrum remains highly correlated with HD.
HD + 2%OC + 0.5%MA + 3%MFA	0.029	0.022	0.95	415.28	14	Combined additives yield a significant area increase and moderate deviation.

Samples containing the OC additive exhibit a pronounced peak around 1030 cm^{-1}, corresponding to the S=O stretching of sulfoxide groups [52]. This peak is a recognised marker for oxidation; its presence in OC-modified binders suggests that OC either introduces sulphur-bearing species or promotes oxidation. Importantly, increases in the sulfoxide (S=O) and carbonyl (C=O) regions should be interpreted cautiously. These bands are widely used as indices of oxidative ageing in bitumen. In more detail, surface-sensitive

spectroscopy studies have shown that oxidised sulphur- and carbon-containing compounds can increase under mild heating and UV irradiation, with negative consequences in terms of surface adhesion [53]. Therefore, the FTIR results above are interpreted as evidence of chemical change (additive-derived and/or oxidation-related) rather than direct proof of enhanced or reduced long-term durability. The literature notes that the sulfoxide index increases with ageing rather than additives [54], so the peak may also signal accelerated oxidative interactions during blending. The MA-modified spectra show increased absorbance near 1695–1730 cm^{-1}. Unaged bitumen normally exhibits a weak carbonyl peak around 1695 cm^{-1} [52]. Maleic anhydride produces strong peaks at 1850, 1780, and 1730 cm^{-1}, which explains the moderate RMSD and MAD values of MA-containing samples. The combination of MA with OC or MFA further strengthens these carbonyl bands. The HD spectrum and several modified spectra display peaks between 450 and 470 cm^{-1}. These correspond to bending vibrations of Si–O–Si and O–Si–O groups in silica or aluminosilicate fillers [55,56]. Their prominence in the HD reference implies that the base binder already contains a micro-filler component, and the peaks intensify in MFA-containing samples, confirming the inclusion of silica-rich materials. It is observed that the wavenumber ~2300–2380 cm^{-1} region appears in the modified bitumen sample but not in the unmodified one; several possible reasons arise. Based on typical FTIR interpretation, that band in most FTIR cases is attributed to ambient CO_2, especially the strong asymmetric stretch near ~2350 cm^{-1} [57]. The peak observed around 2350 cm^{-1} in the modified bitumen may be due to CO_2 adsorption or trapping inside the material. Some additives used for modification, such as porous, mineral, or amine-based materials, can hold small amounts of CO_2 on their surfaces [58]. This can produce a real absorption band near 2350 cm^{-1}. Such behaviour is common in materials that can adsorb gases, like minerals or catalysts, and may also happen in modified bitumen. Therefore, the presence of this peak in the modified sample may result from CO_2 trapped by the additive, not just from air in the instrument.

3.5.2. Comparison of B50/70 and HD

To understand the differences between the reference binders, the 50/70 spectrum was compared directly with the HD spectrum. Table 8 summarises their metrics (both directions are shown because area and peak counts depend on the test spectrum). The HD binder has a larger area and more peaks, indicating a richer chemical composition. Both binders display strong bands at 2920 and 2850 cm^{-1} (asymmetric and symmetric $–CH_2$ stretch) and at 1455 and 1375 cm^{-1} ($–CH_2$/$–CH_3$ bending) [52]. These peaks reflect the long-chain hydrocarbon backbone, common to all bitumen. The HD spectrum shows a subtle 1030 cm^{-1} band and a weak 1695 cm^{-1} band, while the 50/70 binder does not. According to FTIR studies, the sulfoxide peak at 1030 cm^{-1} and the carbonyl peak at 1695 cm^{-1} are markers of oxidation [52]. Their presence in HD suggests that this binder may contain oxidised components or sulphur-bearing additives. HD exhibits a distinct band between 450 and 470 cm^{-1} linked to silica fillers [55,56]. This band is absent in 50/70 binder, indicating that the HD product incorporates inorganic micro-fillers, which can enhance rutting resistance and durability. The 50/70 binder's spectrum contains six prominent peaks, whereas HD has nine. The additional peaks in HD align with silica-related vibrations and weak oxidative bands, supporting the interpretation that HD is a more complex, possibly polymer- modified, binder.

Overall, the analysis of the FTIR dataset with HD as a reference shows distinct additive effects. OC increases total absorbance and introduces a sulfoxide band at 1030 cm^{-1}, while MA produces strong carbonyl peaks near 1730 cm^{-1}. MFA mainly intensifies peaks and adds low-wavenumber silica bands, keeping spectra close to HD. Combined additives yield cumulative effects, with OC + MFA showing the highest peak count. Compared to

50/70, HD binder displays greater absorbance, more peaks, and silica vibrations, indicating a complex, polymer-modified system, whereas 50/70 remains simpler with fewer functional groups.

Table 8. Metrics for the 50/70 vs. HD comparison.

Reference	Test	RMSD	MAD	Corr	Area (AU·cm^{-1})	Peaks	Notes
HD	50/70	0.02665	0.01976	0.853	279.68	11	(1)
50/70	HD	0.02665	0.01976	0.853	334.58	15	(2)

(1) The 50/70 binder has around 17% lower total absorbance and fewer peaks than HD. Major bitumen peaks at 2920 and 2850 cm^{-1} are present, but HD shows additional low-wavenumber Si–O–Si bands and slightly stronger carbonyl and sulfoxide signals. (2) When HD is the test spectrum, the area is higher and more peaks (nine) are detected, reflecting the presence of silica fillers and additional functional groups not found in 50/70.

3.6. Pearson Analyses

The Pearson correlation matrices presented in Figure 13a,b provide valuable insights into the linear relationships between variables, highlighting significant trends between reference and modified bitumen and their rheological behaviour. The following variables are considered: HD: percentage of HD; HD*OC: bitumen modified with organic compound; HD*MA: bitumen modified with multi-functional additive; HD*MFA: bitumen modified with modified filamentous additive; HD*OC*MA: combined modification with organic and multi-functional additives; HD*OC*MFA: combined modification with organic and modified filamentous additives; HD*MA*MFA: combined modification with multi-functional and modified filamentous additives; and HD*OC*MA*MFA: combined modification with all three additives. The heat maps were constructed by scaling Pearson correlation coefficients (r) from −1 (strong negative correlation, shown in blue) to +1 (strong positive correlation, shown in red), as illustrated in Figure 13.

Only the reference HD bitumen exhibited negative correlations with viscosity across all temperatures, with the strongest relationship observed at 100 °C (r = −0.92). In contrast, the OC additive exhibited stronger positive correlations with viscosity among all additives, particularly at 150 °C (r = 0.63). This behaviour indicates that OC-blended mixtures may allow reduced mixing and compaction temperatures, an effect that was especially pronounced in the HD*OC*MA*MFA mixture at 150 °C (r = 0.99). Despite these differences, all additives generally increased viscosity, which is associated with improved resistance to rutting and permanent deformation, particularly at 60 °C.

The weak correlation of HD with G* can be attributed to its inherent stiffness, which limits viscoelastic deformation across temperature variations. By contrast, the moderate correlation between HD and δ at higher temperatures indicates binder softening, which enhances viscoelastic response. At lower temperatures, stiffness dominates, resulting in weaker correlations with δ. Interestingly, while a positive relationship was observed only between HD bitumen G* and phase angle, the incorporation of additives reversed this trend, yielding negative correlations for both G* and δ. These negative correlations became more evident at elevated temperatures (60–90 °C). The most significant case was found in HD*OC interactions, where a strong negative correlation with phase angle was recorded (r = −0.81). This suggests that OC significantly disrupted the network structure and phase stability of HD, resulting in reduced shear resistance and viscoelasticity. Consequently, mixtures containing OC exhibited a greater reduction in phase angle than other mixtures, contributing to an elastic storage modulus. Abe, et al. [59] emphasized that biomaterials used as additives can decrease bitumen stiffness while improving flexibility through network modifications.

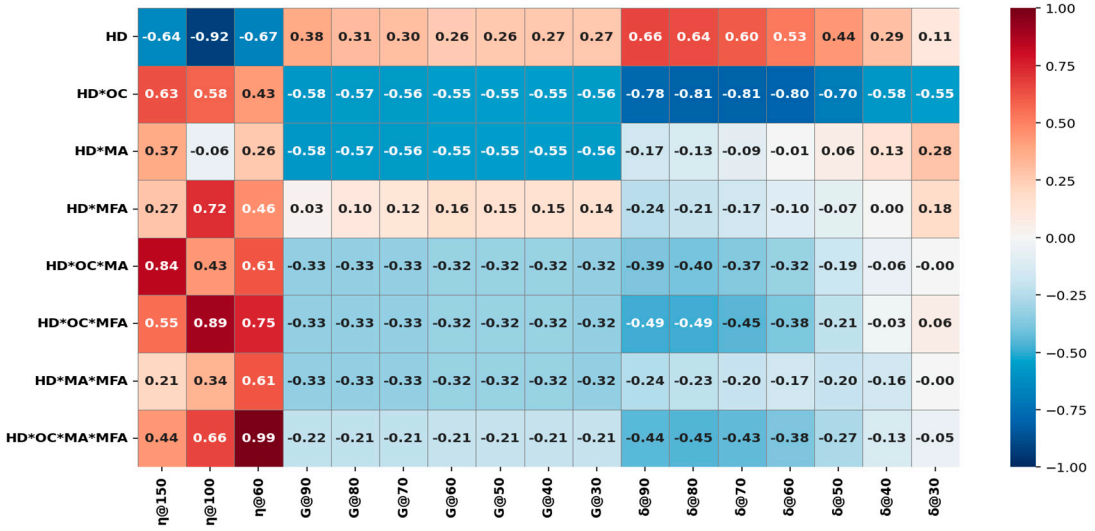

(**a**)

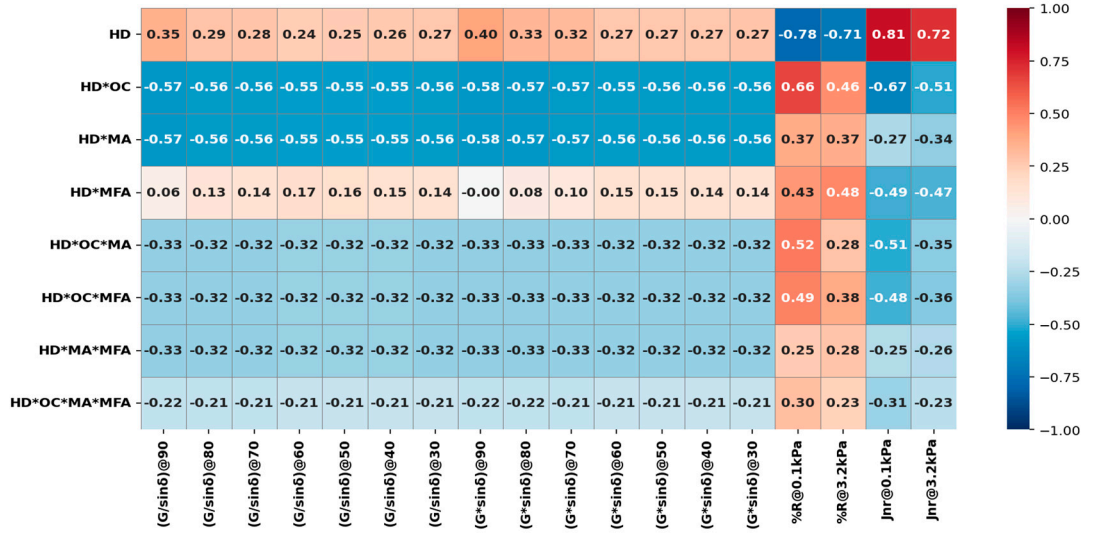

(**b**)

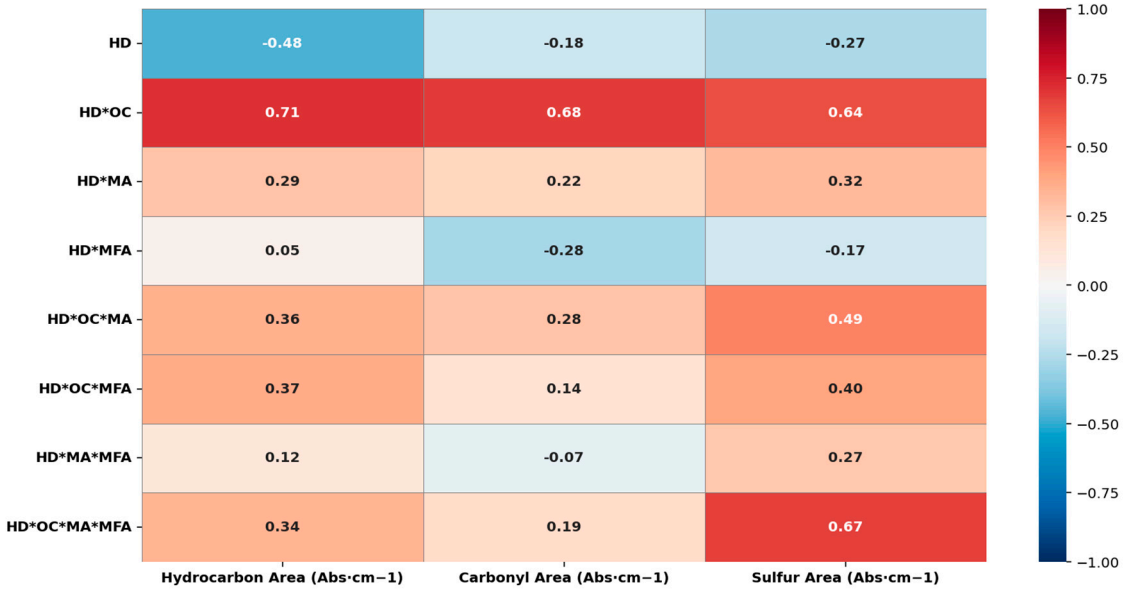

(**c**)

Figure 13. Pearson correlation: (**a**) rheological properties (η, G* and δ); (**b**) performance indicators (G*/sinδ, G*sinδ, R% and Jnr); (**c**) FTIR chemical indices.

In terms of MSCR parameters, reference HD bitumen showed strong negative correlations with percent recovery (R%) (r = −0.78 and r = −0.71) and strong positive correlations with non-recoverable creep compliance (Jnr) (r = 0.81 and r = 0.72). These relationships indicate poor elastic recovery and higher susceptibility to permanent deformation, explaining the greater rutting and fatigue vulnerability of the unmodified binder. The incorporation of most additives, except MFA, reversed these trends by producing positive correlations with R% and negative correlations with Jnr. The most pronounced improvements were observed for HD*OC and HD*MA mixtures individually, whereas the combined HD*OC*MA*MFA system provided only limited enhancement in rutting and fatigue resistance. This highlights the nonlinear and sometimes antagonistic interactions that can arise when multiple additives are used simultaneously, emphasizing the need for careful selection and proportioning to balance stiffness and elasticity.

Figure 13c presents the Pearson correlation coefficients linking the FTIR absorbance areas (hydrocarbon, carbonyl, sulphur) with different binder/additive combinations (HD, HD*OC, HD*MA, HD*MFA, etc.). For the hydrocarbon region, the HD*OC blend shows a strong positive correlation ($r \approx +0.71$), whereas HD alone shows a moderately negative correlation ($r \approx -0.48$). In the carbonyl region, again the HD*OC case dominates with $r \approx +0.68$, while HD*MFA has a modest negative correlation ($r \approx -0.28$). In the sulphur region, the largest positive correlation occurs for HD*OC*MA*MFA ($r \approx +0.67$), whereas HD*MFA alone is slightly negative ($r \approx -0.17$).

These patterns suggest that the organic compound additive (OC) significantly increases aliphatic C–H content (hydrocarbon band) yet also correlates with stronger oxidation signals (carbonyl and sulfoxide bands). This supports the view that oxidation products (C=O, S=O) can be tracked via FTIR indices, as shown by Nie, et al. [60], who found that normalised A_{1700} and A_{1030} (carbonyl and sulfoxide indices) reliably reflect binder ageing. In contrast, the modified filamentous additive (MFA) tends to suppress the carbonyl and sulfoxide responses (negative or weak correlations), implying a potential anti-oxidation effect; this is in line with Maciejewski, et al. [61] who observed certain additives reduce carbonyl/sulfoxide growth. The four-way mix (OC + MA + MFA) shows enhanced sulphur-region correlation but less so carbonyl, hinting at a complex interplay where sulphur-bearing functional groups dominate the oxidation signature in that system. Overall, OC intensifies FTIR ageing markers, MFA moderates oxidation, and combined additives alter the dominant chemical ageing pathways, in agreement with established FTIR-based ageing indicators [60,62].

3.7. Ranking of Blends

In order to rank the mixtures from an ideal standpoint, the following considerations were taken into account (cf. Tables 9 and 10):

- The R%@3.2kPa, % = EL, elasticity (cf. Table 9), recovery at high temperatures, which represents the elasticity of the blend, should be maximised (as per FHWA-HIF-11-038, Table 3). This complies with the specification limits summarised above.
- The ratio, G/sinδ@high temperature = RR, rutting resistance, which is inversely proportional to the work dissipated per load cycle (for a given stress applied during load cycle), should be maximised in order to have a better rutting resistance and a lower dissipated work. This complies with the PG bitumen chart (ASTM D6373, Standard Specification for Performance-Graded Asphalt Binder).
- The product G*sinδ (medium temperatures), which is proportional to the work dissipated per load cycle (for a given constant strain γ = 1.59 Hz applied during load cycle), should be minimised in order to have a better fatigue resistance and a lower dissipated work. Conversely, $(G^*\sin\delta)^{-1}$ = FR, fatigue resistance, should be maximised.

This partly complies with the PG bitumen chart (ASTM D6373), where the boundary condition refers to PAV-aged binder.

- The mixing temperature, which is proportional to CO_2e emissions, should be minimised, for environmental concerns [63]. Conversely, T^{-1} = SU, sustainability, should be maximised.
- The Jnr-diff (percent difference in non-recoverable creep compliance, at high temperatures), which expresses an increase in the plastic percentage with stress, should be minimised to ensure an asphalt binder has low stress sensitivity and will not exhibit excessive permanent deformation (rutting) under heavy traffic loads. This complies with FHWA-HIF-11-038, AASHTO TP70, Standard Method of Test for Multiple Stress Creep Recovery (MSCR) Test of Asphalt Binder Using a Dynamic Shear Rheometer (DSR), and AASHTO MP19 (AASHTO MP 19-10, Standard Specification for Performance-Graded Asphalt Binder Using Multiple Stress Creep Recovery (MSCR)). Conversely, $(\text{Jnr-diff})^{-1}$ = LS, low stress sensitivity, should be maximised.

Table 9. Standardised performance indicators and scores for different asphalt binder blends.

Blends	Indicators					Standardized Indicators					Ranking	
	EL	RR	FR	SU	LS	EL	RR	FR	SU	LS	RA	RB
B50/70	2.14	5.05×10^{2}	2.07×10^{-6}	0.01	5	-	-	0.51	1.00	0.18	0.34	0.29
HD	50.04	1.63×10^{7}	5.37×10^{-10}	0.01	3	0.51	0.65	0.00	0.34	0.15	0.33	0.41
HD + 2OC	87.80	6.73×10^{3}	2.48×10^{-6}	0.01	−5	0.92	0.00	0.61	0.41	0.05	0.40	0.34
HD + 0.5MA	87.36	1.78×10^{3}	3.94×10^{-6}	0.01	−2	0.91	0.00	0.97	0.36	0.08	0.47	0.34
HD + 3MFA	89.18	2.50×10^{7}	3.33×10^{-10}	0.01	−3	0.93	1.00	-	0.26	0.07	0.45	0.57
HD + 2OC + 0.5MA	91.04	2.79×10^{3}	3.90×10^{-6}	0.00	2	0.95	0.00	0.96	-	0.13	0.41	0.27
HD + 2OC + 3MFA	95.64	3.16×10^{3}	3.11×10^{-6}	0.01	−9	1.00	0.00	0.77	0.09	-	0.37	0.27
HD + 0.5MA + 3MFA	90.89	1.95×10^{3}	4.06×10^{-6}	0.01	−2	0.95	0.00	1.00	0.26	0.08	0.46	0.32
HD + 0.5MA + 2OC + 3MFA	93.99	4.25×10^{3}	2.86×10^{-6}	0.01	71	0.98	0.00	0.71	0.04	1.00	0.55	0.51

Symbols: EL = R%@3.2 kPa, elasticity; RR = (G*/sinδ)@80 °C, rutting resistance; FR = (G*sinδ), fatigue resistance; SU = T^{-1}, sustainability; LS = 1/Jnr-diff, low stress sensitivity, RA = ranking considering all the five indicators; RB = ranking considering four indicators (No FR).

Table 10. One-parameter ranking.

	Elasticity	Rutting	Fatigue	Sustainab.	Low Stress Sensitivity
	R%@3.2kPa	(G*/sinδ)@80	1/(G*sinδ)@30	$1/T_{mix}$	1/Jnr-diff
1st Best	HD + 2%OC + 3%MFA	HD + 3% MFA	HD + 0.5%MA + 3%MFA	50/70	HD + 0.5%MA + 2%OC + 3%MFA
2nd	HD + 0.5%MA + 2%OC + 3%MFA	HD	HD + 0.5%MA	HD + 2%OC	50/70
3rd	HD + 2%OC + 0.5%MA	HD + 2%OC	HD + 0.5%MA + 2%OC	HD + 0.5%MA	HD
4th	HD + 0.5%MA + 3%MFA	HD + 0.5%MA + 2%OC + 3%MFA	HD + 2%OC + 3%MFA	HD	HD + 2%OC + 0.5%MA
5th	HD + 3%MFA	HD + 2%OC + 3%MFA	HD + 0.5%MA+ 2OC + 3%MFA	HD + 0.5%MA + 3%MFA	HD + 0.5%MA + 2%OC
6th	HD + 2%OC	HD + 2%OC + 0.5%MA	HD + 2%OC	HD + 3%MFA	HD + 0.5%MA
7th	HD + 0.5%MA	HD + 0.5%MA + 3%MFA	50/70	HD + 2%OC + 3%MFA	HD + 3%MFA
8th	HD	HD + 0.5%MA	HD	HD + 0.5%MA + 2%OC + 3%MFA	HD + 2%OC
9th worst	50/70	50/70	HD + 3%MFA	HD + 2%OC + 0.5%MA	HD + 2%OC + 3%MFA

Under these hypotheses, the ranking can be carried out through an equal-weight multicriteria process, where the indicators above are considered (first matrix), standardised through a max–min procedure, and a score (running sum) is derived (Table 9). Under these hypotheses, the ranking is as follows (ranking A, RA):

$$\text{HD + 0.5MA +2OC + 3MFA > HD + 0.5MA > HD + 0.5MA + 3MFA > HD + 3MFA > HD + 2OC + 0.5MA> HD + 2OC > B50/70 > HD}$$

The ranking RA is based on the assumptions that fatigue is inversely proportional to G*sinδ and that lower mixing temperatures enhance sustainability. However, fatigue specifications apply to aged asphalt (after PAV), while the current study uses unaged binder. Excluding fatigue, the supplementary ranking, RB (cf. Table 9), identifies HD + 3%MFA and, again, HD + 0.5%MA + 2%OC + 3%MFA as optimal and HD + 2%OC + 0.5%MA and HD + 2%OC + 3%MFA as least effective (Table 10). MA primarily reduces mixing temperatures and enhances binder–aggregate adhesion, emphasising that binder-only evaluation of MA-containing blends is insufficient.

It is noted that (1) HD ranks among the worst in terms of elasticity and fatigue resistance. While the need for further investigations for fatigue resistance was discussed above, the unsatisfactory % elastic recovery for a blend with an elastic recovery higher than 80% (RE = d/L, cf. EN 13398) poses some issues on the real significance of the R% as per FHWA-HIF-11-038/AASHTO TP70/AASHTO MP19 and the correlation between these two indicators of elasticity. (2) The "plain" B50/70 seems to have only two points of strengths, i.e., low mixing temperature and low susceptibility to load change. (3) The blend containing the organic compound and the fibres, though resulting in the worst blend for load susceptibility, is on average in the middle of the ranking. (4) The addition of fibres implies a high resistance to rutting, which complies with a lower sustainability when the mixing temperature is considered.

3.8. Mechanistic Interpretation and Limitations

The observed rheological changes can be interpreted through at least four concurrent mechanisms:

(1) Creation of a three-dimensional network due to the addition of polymers. This mechanism is out of scope for this study and gives bitumen the ability to stretch and recover (EL, cf. Table 9), thereby performing better under traffic loads and extreme temperatures than unmodified bitumen (RR, cf. Table 9). At the same time, this implies the need for higher production temperatures and, consequently, lower sustainability (SU, cf. Table 9).

(2) Compositional/phase modification of the maltene–asphaltene balance. This mechanism could be based on the composition of OC, able to act on HD asphaltenes, modify the asphaltene–maltene balance, and increase stiffness and viscosity (cf. Table 9). This is consistent with Cuadri Vega, et al. [64].

(3) Formation of a reinforcing micro-network. This is linked to MFA (which implies high elasticity, cf. Table 9), to MFA + MA (which leads to high elasticity and fatigue resistance, cf. Table 9), and to MFA + MA + OC (which implies high elasticity, high fatigue resistance, and low stress sensitivity, cf. Table 9). In more detail, MFA (alone) produces the largest stiffness/viscosity increase and the highest rutting resistance across 30–90 °C, indicating a dominant reinforcement mechanism. When coupled with OC and MA, this can create a three-dimensional network that restricts shear deformation, leading to increased G* and lower Jnr (cf. Table 9).

(4) Enhanced polar interactions linked to surfactants (MA, with polar head and non-polar tail) and the consequent ability to bond with bitumen polar groups (where HD

asphaltenes and resins play an important role), which increases recoverable response. The same presence of MA seems to imply (cf. Table 9) higher elasticity (even though this is mainly controlled by HD) and fatigue resistance.

In order to better analyse the results, the following observations must be considered:

(A) Overall, the ternary blend achieved the lowest Jnr and very high R%, suggesting that MFA provides the backbone network, while OC and MA improve compatibility and stress-recovery behaviour, resulting in a combined system with both high stiffness and high recoverability. This explains why the ternary formulation outperformed single-additive binders in MSCR performance and provided a balanced ranking when multiple performance indicators were considered.

(B) At the same time, while OC/MA/MFA improved high-temperature rheology and MSCR performance, waste-derived modifiers may introduce trade-offs that should be acknowledged. First, the increased viscosity and mixing/compaction temperatures observed for several blends can raise energy demand and production emissions and may reduce constructability if temperature control is insufficient. Second, the higher stiffness and lower penetration associated with some formulations may increase susceptibility to low-temperature or thermal cracking, especially for hard binders used in climates with large temperature gradients.

(C) From a durability standpoint, improved rutting resistance does not necessarily imply improved moisture damage resistance. Therefore, moisture susceptibility should be verified using mixture-level tests (e.g., ITSR/TSR, Hamburg wheel-tracking in water, or boiling test/rolling bottle test for binder–aggregate adhesion).

(D) OC, MA, and MFA appear difficult to exhibit leaching behaviour. To address this improbable occurrence, leachate testing (e.g., EN 12457 or TCLP-type screening adapted to asphalt materials) is recommended, together with ecotoxicity screening where required by local regulation.

(E) The high stiffness and low Jnr values observed for MFA-containing and ternary blends indicate excellent resistance to permanent deformation at elevated temperatures. However, increased stiffness could also elevate brittleness and cracking susceptibility under cyclic loading and/or at low to intermediate temperatures. Although in the present study fatigue was discussed using binder parameters from unaged DSR sweeps (e.g., G*sinδ), standard fatigue specifications are commonly assessed on aged binders and/or through dedicated damage tests. Therefore, future work should include short- and long-term ageing (RTFOT and PAV) followed by cracking/fatigue characterisation using tests such as LAS (fatigue life), DENT (ductility/strain tolerance), and low-temperature rheology (e.g., BBR where applicable), complemented by mixture-level cyclic fatigue (4PB/SCB) to verify that rutting gains do not compromise cracking performance.

(F) Regarding ageing, FTIR results indicated changes in the carbonyl- and sulfoxide-related regions of the modified binders. However, FTIR analysis alone does not demonstrate either long-term ageing resistance or weakness. Consequently, it is necessary to evaluate whether the additives increase oxidation susceptibility under RTFOT and PAV ageing, as well as under UV exposure representative of service conditions.

(G) At the same time, because the proposed ternary system targets railway waterproofing and sub-ballast applications, durability must also be considered in terms of (i) resistance to moisture ingress and loss of adhesion at the binder–aggregate interface and (ii) resistance to oxidative-driven ageing (and UV-driven near-surface regions). The present work provides binder-level rheological indicators (G*, δ, MSCR) and FTIR fingerprints, which are necessary but not sufficient for quantifying moisture-damage resistance. From a mechanistic standpoint, two opposite mechanisms can

be pointed out: (1) The MA additive is expected to influence binder–aggregate adhesion by modifying interfacial polarity and wettability. Therefore, MA may improve initial adhesion and reduce water displacement potential, particularly on mineral aggregates. (2) At the same time, FTIR changes in the carbonyl/sulfoxide regions are consistent with oxidation-related chemical evolution; such oxidation products could alter acid–base interactions, contributing to adhesion loss under water and environmental exposure, based on binder chemistry and aggregate type. The literature on surface-sensitive spectroscopy also indicates that oxidised sulphur- and carbon-containing compounds may accumulate near the binder surface under environmental exposure and that strong surface oxidation can coincide with a pronounced drop in adhesion after UV exposure. Therefore, to avoid over-interpretation, the expected performance of the ternary binder should be verified through a combined program including (a) short- and long-term ageing (RTFOT and PAV), complemented, where relevant, by UV ageing of thin films; (b) binder–aggregate adhesion testing before and after conditioning (rolling bottle/boiling tests, pull-off/surface energy methods); and (c) mixture-level moisture susceptibility tests (e.g., ITSR/TSR and/or Hamburg wheel-tracking in water). These tests will clarify whether the observed binder-level rutting resistance gains translate into improved long-term waterproofing performance without moisture-induced debonding.

4. Conclusions

This study examined the improvement of HD bitumen rheological properties at medium-to-high temperatures through incorporating OC, MA, and MFA, using waste-derived additives aimed at railway waterproofing and sub-ballast applications. The key conclusions reached are listed below.

- Time-dependent flow behaviour results indicate that adding OC to HD mixtures may reduce mixing and compaction temperatures, while MFA can increase them. Overall, the higher viscosity of modified HD bitumen may necessitate a wider range of mixing and compaction temperatures, requiring greater energy input and more precise temperature control in both mixing plants and road applications.
- Oscillation test results conducted at elevated temperatures (up to 90 °C) showed that HD bitumen had significantly increased rutting resistance compared to B50/70 bitumen, as evidenced by increased G* and lower δ values. Moreover, it is interesting that all additives caused a decrease in δ values after the test temperature exceeded 40 °C. In other words, the modified mixtures exhibited a more elastic behaviour. At all temperatures, the addition of MFA provided a more stable structure according to the base matrix.
- During the creep-recovery periods of the MSCR test, MFA increased the viscoelastic response, OC reduced temperature sensitivity, and MA improved rutting performance by increasing the mix's stiffness at elevated temperatures. Consequently, the mix modified with OC, MA, and MFA demonstrated improved shear resistance with lower Jnr values, and R% values increased by around 40% compared to HD bitumen. As a result, the HD + 2%OC + 0.5%MA + 3%MFA mix combined elasticity and stiffness to enhance both rutting and fatigue resistance, providing a more balanced temperature-dependent performance.
- FTIR analysis confirmed that the HD binder exhibits a more complex and oxidized chemical structure than the 50/70 base binder, characterized by stronger carbonyl-, sulfoxide-, and silica-related peaks, indicating polymer modification.
- FTIR analyses indicated that OC-, MA-, and MFA-containing blends exhibit changes in polar functional groups, including stronger absorbance in the carbonyl (~1700 cm^{-1})

and/or sulfoxide (~1030 cm^{-1}) regions and low-wavenumber silica-related vibrations. Even if carbonyl and sulfoxide bands are commonly associated with oxidation/ageing markers, these FTIR observations cannot be interpreted either as improved or as reduced durability. Rather, they indicate chemical modifications and/or oxidation-related changes that must be validated through dedicated ageing and moisture/adhesion testing.

Overall, the experimental results show that while each organic-based waste additive enhances HD bitumen performance individually, their combined use offers superior rutting and fatigue resistance. This supports the application of modified HD bitumen in railway systems, though further studies are needed on long-term cyclic loading, ballast interaction, and environmental sustainability. Interestingly, bitumen with high softening points and very low Jnr values exhibited negative Jnr-diff, contrary to the literature, suggesting complex behaviour under stress. As network integrity depends on stress amplitude, further investigation is warranted. These findings establish a foundation for advancing high-performance, durable railway bituminous systems. Because the present work is limited to binder-level rheology and FTIR, moisture damage resistance (water stability/stripping) cannot be concluded from these results. A dedicated verification through mixture-level moisture susceptibility (e.g., ITSR/TSR or Hamburg wheel-tracking in water) and/or binder–aggregate adhesion tests (e.g., rolling bottle or boiling test) is recommended as the next step.

Author Contributions: Conceptualization, F.G.P., E.E. and V.N.K.M.; data curation, F.G.P., E.E. and V.N.K.M.; formal analysis, F.G.P., E.E. and V.N.K.M.; investigation, F.G.P., E.E. and V.N.K.M.; methodology: F.G.P., E.E. and V.N.K.M.; validation, F.G.P., E.E. and V.N.K.M.; visualisation, E.E. and V.N.K.M.; writing—original draft preparation, E.E. and V.N.K.M.; writing—review and editing, F.G.P.; funding acquisition, F.G.P.; project administration, F.G.P.; Resources, F.G.P.; Supervision, F.G.P. All authors have read and agreed to the published version of the manuscript.

Funding: This study was carried out within the MOST—Sustainable Mobility National Research Center and received funding from the European Union Next-GenerationEU (PIANO NAZIONALE DI RIPRESA E RESILIENZA (PNRR)—MISSIONE 4 COMPONENTE 2, INVESTIMENTO 1.4—D.D. 1033 17 June 2022, CN00000023). This manuscript reflects only the authors' views and opinions. Neither the European Union nor the European Commission can be considered responsible for them. Furthermore, because of the interaction with other studies, the authors would like to thank also (1) Eng. Giuseppe Colicchio. (2) The European Commission for its financial contribution: (2.1) to the LIFE SILENT project "Sustainable Innovations for Long-life Environmental Noise Technologies" (LIFE22-ENV-IT-LIFE-SILENT/101114310 | Acronym: LIFE22-ENV-IT-LIFE SILENT). (2.2) to the LIFE SNEAK Project "optimised Surfaces against NoisE And vibrations produced by tramway tracK and road traffic" (LIFE20 ENV/IT/000181 | Acronym: LIFE SNEAK).

Data Availability Statement: The raw data supporting the conclusions of this article will be made available by the authors on request.

Acknowledgments: The authors would like to thank all those who supported them with this research, especially the European Commission and Giuseppe Colicchio.

Conflicts of Interest: The authors declare no conflict of interest.

References

1. Bosso, N.; Magelli, M.; Zampieri, N. Dynamical effects of the increase of the axle load on European freight railway vehicles. *Appl. Sci.* **2023**, *13*, 1318. [CrossRef]
2. Na, I.; Park, H.; Yun, J.; Park, J.D.; Kim, H. Characterization of Asphalt Binder and Mixture for Enhanced Railway Applications. *Materials* **2025**, *18*, 3265. [CrossRef] [PubMed]

3. Liu, Z.; Hong, J.; Liu, J. Rheological behavior of fresh cement asphalt mortar. In *Sustainable Construction Materials 2012*; ASCE: Reston, VA, USA, 2012; pp. 54–63.
4. Xiao, X.; Cai, D.; Lou, L.; Shi, Y.; Xiao, F. Application of asphalt based materials in railway systems: A review. *Constr. Build. Mater.* **2021**, *304*, 124630. [CrossRef]
5. Castro, G.; Pires, J.; Motta, R.; Bernucci, L.; Fortunato, E.; Futai, M. Evaluating environmental effects on the structural behavior of the railroad track subgrade considering different sub-ballast design solutions. *Transp. Geotech.* **2022**, *34*, 100761. [CrossRef]
6. Cao, J.; Wang, L. Mechanistic Study on the Optimization of Asphalt-Based Material Properties by Physicochemical Interaction and Synergistic Modification of Molecular Structure. *Polymers* **2024**, *16*, 2924. [CrossRef]
7. Martinez-Toledo, C.; Valdes-Vidal, G.; Calabi-Floody, A.; Gonzalez, M.E.; Reyes-Ortiz, O. Evaluation of Rheological Properties of Asphalt Binder Modified with Biochar from Oat Hulls. *Materials* **2024**, *17*, 4312. [CrossRef]
8. Sukkari, A.; Al-Khateeb, G.; Zeiada, W.; Ezzat, H. Evaluation of aging impact on rheological and chemical characteristics of crumb rubber-modified warm asphalt binders. *Sci. Prog.* **2024**, *107*, 00368504241300198. [CrossRef] [PubMed]
9. Alas, M.; Albrka, S.I.; Eltwati, A.; Ali, A.S.B.; Al Allam, A.M. Analysis of the Optimum Performance for Polymer and Polymer–Nanocomposite-modified Asphalt by Using Multicriteria Decision Analysis. *Polymers* **2024**, *16*, 3128. [CrossRef]
10. Huang, B.; Wang, C.; Yang, Y.; Wang, Y.; Zhao, Y.; Jiang, R. Research on component compatibility and aging behavior of chemically toughened high-performance asphalt. *Front. Built Environ.* **2025**, *11*, 1638263. [CrossRef]
11. Farrar, M.; Sui, C.; Salmans, S.; Qin, Q. Determining the low-temperature rheological properties of asphalt binder using a dynamic shear rheometer (DSR). *Rep. 4FP* **2015**, *8*, 20.
12. Peng, J.; Deng, D.; Liu, Z.; Yuan, Q.; Ye, T. Rheological models for fresh cement asphalt paste. *Constr. Build. Mater.* **2014**, *71*, 254–262. [CrossRef]
13. Sybilski, D. Relationship between absolute viscosity of polymer-modified bitumens and rutting resistance of pavement. *Mater. Struct.* **1994**, *27*, 110–120. [CrossRef]
14. Morea, F.; Agnusdei, J.O.; Zerbino, R. The use of asphalt low shear viscosity to predict permanent deformation performance of asphalt concrete. *Mater. Struct.* **2011**, *44*, 1241–1248. [CrossRef]
15. Li, J.; Li, Y.; Li, M.; Lu, H.; Cao, D. Dynamic viscosity standard of high viscosity modified asphalt considering temperature and load coupling effect. *IOP Conf. Ser. Mater. Sci. Eng.* **2021**, *1075*, 012013. [CrossRef]
16. D'Angelo, J.A. MSCR: What Is Jnr Diff and What Does It Mean? *Asph. Mag.* **2018**, *Fall 2018*, 36–38.
17. Arafat, S.; Noor, L.; Wasiuddin, N.M.; Salomon, D. Development of a test method to measure RAP percentage in asphalt mixes in the field using a handheld FT-IR spectrometer. *J. Mater. Civ. Eng.* **2020**, *32*, 04020352. [CrossRef]
18. Yegane, M.; Katanalp, B.Y.; Ahmedzade, P. Effects of using biochar materials obtained from cherry and sour cherry wastes on bitumen modification. *Constr. Build. Mater.* **2025**, *470*, 140609. [CrossRef]
19. Dyuryagina, A.; Byzova, Y.; Ostrovnoy, K.; Demyanenko, A.; Tyukanko, V.; Lutsenko, A. The Effect of the Microstructure and Viscosity of Modified Bitumen on the Strength of Asphalt Concrete. *Polymers* **2024**, *16*, 1370. [CrossRef]
20. Li, C.; Liu, H.; Xiao, Y.; Li, J.; Wang, T.; Peng, L. Modification and enhancing contribution of fiber to asphalt binders and their corresponding mixtures: A study of viscoelastic properties. *Materials* **2023**, *16*, 5727. [CrossRef]
21. Fazaeli, H.; Amini, A.A.; Nejad, F.M.; Behbahani, H. Rheological properties of bitumen modified with a combination of FT paraffin wax (sasobit®) and other additives. *J. Civ. Eng. Manag.* **2016**, *22*, 135–145. [CrossRef]
22. Remisova, E.; Briliak, D.; Holy, M. Evaluation of thermo-viscous properties of bitumen concerning the chemical composition. *Materials* **2023**, *16*, 1379. [CrossRef] [PubMed]
23. Mirsepahi, M.; Tanzadeh, J.; Ghanoon, S.A. Laboratory evaluation of dynamic performance and viscosity improvement in modified bitumen by combining nanomaterials and polymer. *Constr. Build. Mater.* **2020**, *233*, 117183. [CrossRef]
24. Rodríguez-Alloza, A.; Gallego, J. Volumetric characteristics and compactability of asphalt rubber mixtures with organic warm mix asphalt additives. *Mater. Construcción* **2017**, *67*, e123. [CrossRef]
25. Crispino, M.; Mariani, E.; Toraldo, E. Assessment of fiber-reinforced bituminous mixtures' compaction temperatures through mastics viscosity tests. *Constr. Build. Mater.* **2013**, *38*, 1031–1039. [CrossRef]
26. Wang, Y.; Wang, W.; Wang, L. Understanding the relationships between rheology and chemistry of asphalt binders: A review. *Constr. Build. Mater.* **2022**, *329*, 127161. [CrossRef]
27. Isacsson, U.; Lu, X. Characterization of bitumens modified with SEBS, EVA and EBA polymers. *J. Mater. Sci.* **1999**, *34*, 3737–3745. [CrossRef]
28. Lu, X.; Soenen, H.; Redelius, P. Rheological characterization of polymer modified bitumens. *Annu. Trans. Nord. Rheol. Soc.* **2011**, *19*, 77–84.
29. Zhu, J.; Lu, X. Influence of morphology on high-temperature rheological properties of bitumen modified with styrene-butadiene-styrene (SBS) copolymer. *Front. Struct. Civ. Eng.* **2021**, *15*, 806–819. [CrossRef]
30. Fu, Z.; Hou, Y.; Ma, F.; Fu, Z.; Cui, J.; Liu, Z.; Liu, J. Investigation of rheological properties of asphalt modified with low-temperature microencapsulated eutectic phase change materials. *Case Stud. Constr. Mater.* **2024**, *20*, e03201. [CrossRef]

31. Behzadfar, E.; Hatzikiriakos, S.G. Rheology of bitumen: Effects of temperature, pressure, CO_2 concentration and shear rate. *Fuel* **2014**, *116*, 578–587. [CrossRef]
32. Xu, X.; Yuan, L.; Cong, P.; Wang, Z.; Guo, H.; Zhou, X.; Shao, T. Rheological and healing properties of bitumen containing carbon black microcapsules. *Fuel* **2024**, *373*, 132399. [CrossRef]
33. Erkuş, Y.; Kök, B.V.; Yilmaz, M. Evaluation of performance and productivity of bitumen modified by three different additives. *Constr. Build. Mater.* **2020**, *261*, 120553. [CrossRef]
34. Rodríguez-Alloza, A.M.; Gallego, J.; Pérez, I.J.C.; Materials, B. Study of the effect of four warm mix asphalt additives on bitumen modified with 15% crumb rubber. *Constr. Build. Mater.* **2013**, *43*, 300–308. [CrossRef]
35. Porot, L.; Zhu, J.; Wang, D.; Cannone Falchetto, A. Multiple stress creep recovery test to differentiate polymer modified bitumen at high temperature. *J. Test. Eval.* **2023**, *51*, 2168–2178. [CrossRef]
36. Stempihar, J.; Gundla, A.; Underwood, B.S. Interpreting stress sensitivity in the multiple stress creep and recovery test. *J. Mater. Civ. Eng.* **2018**, *30*, 04017283. [CrossRef]
37. Wang, H.; Liu, X.; Apostolidis, P.; Wang, D.; Leng, Z.; Lu, G.; Erkens, S.; Skarpas, A. Investigating the high-and low-temperature performance of warm crumb rubber–modified bituminous binders using rheological tests. *J. Transp. Eng. Part B Pavements* **2021**, *147*, 04021067. [CrossRef]
38. Habbouche, J.; Hajj, E.Y.; Sebaaly, P.E.; Piratheepan, M. A critical review of high polymer-modified asphalt binders and mixtures. *Int. J. Pavement Eng.* **2020**, *21*, 686–702. [CrossRef]
39. Alisov, A.; Riccardi, C.; Schrader, J.; Cannone Falchetto, A.; Wistuba, M.P. A novel method to characterise asphalt binder at high temperature. *Road Mater. Pavement Des.* **2020**, *21*, 143–155. [CrossRef]
40. Adorjányi, K.; Füleki, P. Performance evaluation of bitumens at high temperature with multiple stress creep recovery test. *Hung. J. Ind. Chem.* **2011**, *39*, 195–199.
41. Hossain, Z.; Zaman, M.; Ghosh, D. *Creep Compliance and Percent Recovery of Oklahoma Certified Binder Using the Multiple Stress Recovery (MSCR) Method*; Department of Transportation, Materials and Research Division: Oklahoma, OK, USA, 2015.
42. Wang, D.; Zhu, J.; Porot, L.; Cannone Falchetto, A.; Damen, S. Multiple stress creep and recovery test for bituminous binders–influence of several key experimental parameters. *Road Mater. Pavement Des.* **2023**, *24*, 290–308. [CrossRef]
43. Martín-Alfonso, J.E.; Martín-Alfonso, M.J.; Valencia, C.; Cuberes, M.T. Rheological and tribological approaches as a tool for the development of sustainable lubricating greases based on nano-montmorillonite and castor oil. *Friction* **2021**, *9*, 415–428. [CrossRef]
44. Zeng, G.; Zhang, J.; Huang, H.; Xiao, X.; Yan, C. A comparative study for creep and recovery behavior characterization of modified bitumens using the MSCR test. *Coatings* **2023**, *13*, 1445. [CrossRef]
45. Zhou, S.; Yan, J.; Li, L.; Li, S.; Wu, S.; Yan, C.; Ai, C. Investigating the influence of stress dependency on the evaluation of high-temperature deformation resistance in SBS-modified asphalt. *Constr. Build. Mater.* **2024**, *438*, 137049. [CrossRef]
46. Showkat, B.; Suresha, S.; Akhandappagol, N. Study of rheological and creep recovery properties of asphalt binder modified with waste toner. *J. Mater. Civ. Eng.* **2020**, *32*, 04020331. [CrossRef]
47. Airey, G.; Grenfell, J.; Apeagyei, A.; Subhy, A.; Lo Presti, D. Time dependent viscoelastic rheological response of pure, modified and synthetic bituminous binders. *Mech. Time-Depend. Mater.* **2016**, *20*, 455–480. [CrossRef]
48. Günay, T. Investigation of physical properties of base and SBS modified bitumens by rheological test methods. *Rev. Constr.* **2022**, *21*, 281–294. [CrossRef]
49. Yan, C.; Xi, J.; Ai, C.; Leng, Z. Investigating the unique entropy-elasticity of polymer modified asphalt. *Clean. Mater.* **2024**, *11*, 100216. [CrossRef]
50. Zhu, J.; Lu, X. Effect of Morphology on High-Temperature Rheological Properties of Polymer-Modified Bitumen. In *RILEM 252-CMB-Symposium on Chemo Mechanical Characterization of Bituminous Materials*; Springer International Publishing: Cham, Switzerland, 2018; pp. 99–104.
51. Vernerey, F.J.; Brighenti, R.; Long, R.; Shen, T. Statistical damage mechanics of polymer networks. *Macromolecules* **2018**, *51*, 6609–6622. [CrossRef]
52. Wasiuddin, N.; Hossain, R.; Arafat, S.; Noor, L. *Field Implementation of Handheld FTIR Spectrometer for Polymer Content Determination and for Quality Control of RAP Mixtures*; The National Academies of Sciences, Engineering, and Medicine: Washington, DC, USA, 2022.
53. Hung, A.; Li, M.; Fini, E.H. Effects of elemental sulfur on the aging trajectory and adhesion characteristics of rubber-modified bitumen. *ACS Sustain. Chem. Eng.* **2021**, *9*, 16918–16925. [CrossRef]
54. Iwański, M.; Chomicz-Kowalska, A.; Maciejewski, K.; Iwański, M.M.; Radziszewski, P.; Liphardt, A.; Król, J.B.; Sarnowski, M.; Kowalski, K.J.; Pokorski, P. Effects of laboratory ageing on the FTIR measurements of water-foamed bio-fluxed asphalt binders. *Materials* **2023**, *16*, 513. [CrossRef]

55. Barbosa, S.L.; Ottone, M.; de Almeida, M.T.; Lage, G.L.; Almeida, M.A.; Nelson, D.L.; Dos Santos, W.T.; Clososki, G.C.; Lopes, N.P.; Klein, S.I.; et al. Ketalization of ketones to 1,3-dioxolanes and concurring self-aldolization catalyzed by an amorphous, hydrophilic SiO_2-SO_3H catalyst under microwave irradiation. *J. Braz. Chem. Soc.* **2018**, *29*, 1663–1671. [CrossRef]
56. Nasrazadani, S.; Mielke, D.; Springfield, T.; Ramasamy, N. *Practical Applications of FTIR to Characterize Paving Materials*; The National Academies of Sciences, Engineering, and Medicine: Washington, DC, USA, 2010.
57. Fourier-Transform Infrared Spectroscopy. Available online: https://spectralysbiotech.com/ftir-technology/ (accessed on 4 September 2025).
58. Collins, S.E.; Baltanás, M.A.; Bonivardi, A.L. Infrared spectroscopic study of the carbon dioxide adsorption on the surface of Ga_2O_3 polymorphs. *J. Phys. Chem. B* **2006**, *110*, 5498–5507. [CrossRef]
59. Abe, A.A.; Oliviero Rossi, C.; Caputo, P. Biomaterials and their potentialities as additives in bitumen technology: A review. *Molecules* **2022**, *27*, 8826. [CrossRef]
60. Nie, Y.; Gao, W.; Zhou, C.; Yu, P.; Song, X. Evaluation of ageing behaviors of asphalt binders using FTIR tests. *Int. J. Pavement Res. Technol.* **2021**, *14*, 615–624. [CrossRef]
61. Maciejewski, K.; Chomicz-Kowalska, A.; Bartos, J. Effects of Laboratory Ageing on the Chemical Composition and High-Temperature Performance of Warm Mix Asphalt Binders. *Appl. Sci.* **2024**, *14*, 8524. [CrossRef]
62. Hofko, B.; Alavi, M.Z.; Grothe, H.; Jones, D.; Harvey, J. *Infrared Spectroscopy on Asphalt Binders: Improving Repeatability and Sensitivity*; The National Academies of Sciences, Engineering, and Medicine: Washington, DC, USA, 2018.
63. Liu, Y.; Liu, Z.; Zhu, Y.; Zhang, H. A Review of Sustainability in Hot Asphalt Production: Greenhouse Gas Emissions and Energy Consumption. *Appl. Sci.* **2024**, *14*, 10246. [CrossRef]
64. Cuadri Vega, A.A.; García Morales, M.; Navarro Domínguez, F.J.; Partal López, P. Isocyanate-functionalized castor oil as a novel bitumen modifier. *Chem. Eng. Sci.* **2013**, *97*, 320–327. [CrossRef]